

Optimizing quantum violation for multipartite facet Bell inequalities

Jin-Fu Chen (陈劲夫)^{1, 2, *} Mengyao Hu (胡梦瑶)^{1, 2, †} and Jordi Tura^{1, 2, ‡}

¹*Instituut-Lorentz, Universiteit Leiden, P.O. Box 9506, 2300 RA Leiden, The Netherlands*

² *$\langle aQa^L \rangle$ Applied Quantum Algorithms, Universiteit Leiden, The Netherlands*

(Dated: January 21, 2026)

Nonlocality shapes quantum correlations, revealed through the violation of Bell inequalities. The intersection of all valid Bell inequalities is the so-called local polytope. In multipartite systems, characterizing the local polytope quickly becomes an intractable task as the system size increases. Optimizing Bell inequalities to maximize the ratio between their quantum value and classical bound is key to understanding multipartite nonlocality. We propose a gradient-based method for this optimization. Numerical results indicate that local maxima of this ratio typically correspond to facet Bell inequalities of the local polytope. This enables an iterative search for tight and robust Bell inequalities. Applied to permutation-invariant scenarios, the method provides tight Bell inequalities with large quantum violations and facilitates experimental certification of Bell correlations without full knowledge of the local polytope. Moreover, analytical results of the maximum ratio are derived in the thermodynamic limit.

Introduction.—Bell inequalities serve as fundamental tools for detecting quantum nonlocality, the inability of local hidden variable theories to reproduce all quantum predictions [1, 2]. Among them, the Clauser-Horne-Shimony-Holt (CHSH) inequality is the most studied and experimentally tested Bell inequality [3]. It provides a clear signature of nonlocal correlations in bipartite systems [4, 5], where recent breakthroughs have enabled loophole-free tests [6–10]. Beyond its foundational significance, nonlocality has emerged as a critical resource for device-independent quantum information protocols, including quantum key distribution [11–14], certified randomness generation [15–17], and quantum system verification through self-testing [18–20].

Generalizing Bell nonlocality to the multipartite regime poses significant conceptual and practical challenges. As the number of parties increases, while the settings per party remain fixed, the number of correlation terms grows exponentially, and the complexity of characterizing the local polytope grows as $O((\exp N)^{(\exp N)})$ [21], rendering a complete characterization of multipartite nonlocality intractable [22–24]. The local polytope, defined as the intersection of all valid Bell inequalities [25], can be characterized either by its vertices or its facets. Although generating the vertices is straightforward, the number grows exponentially with the number of parties. Deriving the corresponding facets quickly becomes computationally intractable [21, 26]. A practical approach is to restrict to few-body correlators and exploit symmetries, thereby greatly reducing the number of free coefficients in Bell inequalities and constraining the structure of correlations [27, 28]. For instance, permutation symmetry among parties allows the construction of symmetric Bell inequalities that detect nonlocality in physically relevant many-body systems [29, 30], while remaining analytically and numerically tractable [27, 31]. Symmetry thus provides a promising route to construct scalable and experimentally relevant Bell inequalities for

many-body systems [32, 33].

To characterize multipartite Bell nonlocality, it is essential to optimize Bell inequalities to enhance the gap between the classical bound and the quantum value. Such optimized inequalities are particularly useful in experiments, as larger separation generally implies greater robustness to noise and improved feasibility in experimental implementations [33–35]. In addition to enhancing the quantum–classical gap, identifying tight Bell inequalities that define facets of the local polytope is also important, as they set the fundamental limits of classical correlations, and all facets together form the minimal description of correlations consistent with a local hidden-variable model. However, current methods for identifying these robust and tight Bell inequalities face significant limitations. Recent approaches leveraging machine learning techniques [36] and iterative optimization methods [35] have shown potential, but these methods exhibit limited scalability and fail to characterize complex polytopes.

In this Letter, we propose a gradient-based method to optimize Bell inequalities by enhancing the ratio between the quantum value for a fixed Hilbert space dimension, and the classical bound. We observe that the method converges to a local maximum of this ratio that corresponds to a tight Bell inequality. It simultaneously determines the classical bound, the measurement settings, and the quantum state achieving the quantum violation corresponding to such local maximum. We focus on the $(N, m, 2)$ scenario, where each of the N parties performs one of m possible measurements with binary outcomes ± 1 . As a first benchmark, our optimization reproduces the CHSH inequality in the symmetrized $(2, 2, 2)$ scenario. We then apply it to the permutation-invariant (PI) Bell inequalities consisting of up to two-body correlators for general $(N, m, 2)$ scenarios with $m = 2$ and 3. Our approach avoids enumerating all facets of the corresponding local polytope at once, a task that becomes

intractable due to the exponential complexity with N . We identify families of tight Bell inequalities for $m = 2$ and 3, and obtain previously unknown tight Bell inequalities for $m = 3$. Finally, we verify the maximum ratio on the affine projections and cross sections of both the primal and dual spaces, which reveals geometric insight into multipartite nonlocality. We also obtain analytical results for the maximum ratio in the thermodynamic limit $N \rightarrow \infty$ for small m , while in the combined limit $N, m \rightarrow \infty$ it approaches $\coth(1)$.

Setup.—A Bell inequality is given by a linear functional of the probability distribution $I = \sum_{\mathbf{a}, \mathbf{x}} T_{\mathbf{a}, \mathbf{x}} P(\mathbf{a}|\mathbf{x}) \geq \beta_C$, where the coefficients $T_{\mathbf{a}, \mathbf{x}} \in \mathbb{R}$ specify the inequality, $P(\mathbf{a}|\mathbf{x})$ denotes the conditional probability of obtaining outcomes $\mathbf{a} = (a_1, \dots, a_N)$ with $a_i = 0$ or 1 given measurement settings $\mathbf{x} = (x_1, \dots, x_N)$ with $x_i \in [m] = \{0, \dots, m-1\}$. The classical bound β_C is defined as the minimum of I over all local behaviors, $\beta_C = \min_{\vec{P} \in \mathcal{L}} I$, and $\vec{P} = \{P(\mathbf{a}|\mathbf{x})\}_{\mathbf{a}, \mathbf{x}}$ [37], where \mathcal{L} is the local polytope. The inequality is tight when the saturating local behaviors define a facet of the polytope \mathcal{L} , i.e., a supporting hyperplane of maximal dimension. We reformulate the linear functional in the correlator space as [20]

$$I = \sum_{\boldsymbol{\mu}} \alpha_{\boldsymbol{\mu}} \langle A_{\boldsymbol{\mu}} \rangle, \quad (1)$$

where the composite index $\boldsymbol{\mu}$ labels the ℓ -body correlator $A_{\boldsymbol{\mu}} = A_{x_{i_1}}^{(i_1)} \cdots A_{x_{i_\ell}}^{(i_\ell)}$ acting on the sites i_1, i_2, \dots, i_ℓ with $1 \leq i_1 < i_2 < \cdots < i_\ell \leq N$. The inputs on these sets are given by $\mathbf{x}_\ell = (x_{i_1}, \dots, x_{i_\ell}) \in [m]^\ell$. For binary outcomes, the correlator is defined by $\langle A_{\boldsymbol{\mu}} \rangle = \sum_{\mathbf{a}_\ell} (-1)^{\sum_{j=1}^\ell a_{i_j}} P(\mathbf{a}_\ell|\mathbf{x}_\ell)$ with $\mathbf{a}_\ell = (a_{i_1}, \dots, a_{i_\ell})$. The coefficient of each correlator is given by $\alpha_{\boldsymbol{\mu}} \in \mathbb{R}$. The classical bound of the Bell inequality can be rewritten in correlator form as $\beta_C = \min_{\langle A_{\boldsymbol{\mu}} \rangle \in \mathcal{L}} I$, where \mathcal{L} now denotes the local polytope in the correlator space.

In the quantum case, the linear functional (1) corresponds to the expectation value of Bell operators on a quantum state, and such operators can be interpreted as a Hamiltonian in quantum many-body systems. The spectral properties of these Hamiltonians, in particular their ground state energies, quantify multipartite nonlocality with a fixed Hilbert space dimension [38, 39]. For an N -partite pure $|\psi\rangle$, the expectation of the correlator is given by $\langle \hat{A}_{\boldsymbol{\mu}} \rangle = \langle \psi | \hat{A}_{\boldsymbol{\mu}} | \psi \rangle$. Note that observables $\hat{A}_{\boldsymbol{\mu}}$ are parameterized by the measurement setting $\boldsymbol{\theta} = \{\theta_x^{(i)}\}_{i,x}$ and acts as a Hermitian operator on the Hilbert space with a fixed dimension. By specifying all measurement settings, one defines the Bell operator $\hat{I}(\boldsymbol{\theta})$. The minimum quantum value is obtained by optimizing over all measurement settings and states $\beta_Q = \min_{\boldsymbol{\theta}, |\psi\rangle} \langle \psi | \hat{I}(\boldsymbol{\theta}) | \psi \rangle := \langle \psi^* | \hat{I}(\boldsymbol{\theta}^*) | \psi^* \rangle$, where $|\psi^*\rangle$ is the ground state and $\boldsymbol{\theta}^* = \{\theta_x^{(i)*}\}_{i,x}$ is the optimal measurement setting that minimize the ground-state en-

ergy. To minimize the quantum value β_Q , we compute its gradient with respect to the measurement parameters $\boldsymbol{\theta}$. The derivatives are given by [40]

$$\frac{\partial}{\partial \theta_x^{(i)}} \langle \psi^* | \hat{I}(\boldsymbol{\theta}) | \psi^* \rangle = \langle \psi^* | \frac{\partial \hat{I}(\boldsymbol{\theta})}{\partial \theta_x^{(i)}} | \psi^* \rangle. \quad (2)$$

A Bell inequality is nontrivial if $\beta_Q/\beta_C > 1$, meaning that some quantum states and measurements lead to violations of the classical bound β_C .

Ratio optimization.—We define the ratio $\Delta := \beta_Q/\beta_C$ that characterizes the potential of a Bell inequality to certify nonlocal correlations, with larger values indicating greater robustness to noise. By optimizing the coefficients $\alpha_{\boldsymbol{\mu}}$, we maximize the ratio Δ , and our numerical results indicate that the local maxima typically correspond to facet Bell inequalities.

Note that β_Q is a piecewise-smooth function with respect to the coefficients $\alpha_{\boldsymbol{\mu}}$, and its derivatives are given by [40]

$$\frac{\partial \beta_Q}{\partial \alpha_{\boldsymbol{\mu}}} = \langle \psi^* | \frac{\partial \hat{I}(\boldsymbol{\theta})}{\partial \alpha_{\boldsymbol{\mu}}} \Big|_{\boldsymbol{\theta}=\boldsymbol{\theta}^*} | \psi^* \rangle. \quad (3)$$

For the classical bound β_C , kinks occur when the set of saturating vertices changes on the local polytope. From the definition of β_C , at least one vertex saturates the Bell inequality. We fix the classical bound β_C and iteratively add new saturating vertices determined by the gradient direction of β_Q . The coefficients $\alpha_{\boldsymbol{\mu}}$ are updated along this direction to increase the ratio

$$\frac{\partial \Delta}{\partial \alpha_{\boldsymbol{\mu}}} = \frac{1}{\beta_C} \frac{\partial \beta_Q}{\partial \alpha_{\boldsymbol{\mu}}}, \quad (4)$$

subject to the constraints $\sum_{\boldsymbol{\mu}} \alpha_{\boldsymbol{\mu}} v_{\boldsymbol{\mu},j} = \beta_C$, where $v_{\boldsymbol{\mu},j}$ are the vertices saturating the classical bound. Other vertices yield larger classical values than the classical bound $\sum_{\boldsymbol{\mu}} \alpha_{\boldsymbol{\mu}} \langle A_{\boldsymbol{\mu}} \rangle \geq \beta_C$. By varying $\alpha_{\boldsymbol{\mu}}$, new vertices become active and are added to the constraints, progressively tightening the Bell inequality. A Bell inequality becomes tight when its hyperplane forms a facet of the local polytope, i.e., when it is saturated by a sufficient number of affinely independent vertices. We give the update rule of $\alpha_{\boldsymbol{\mu}}$ in [40].

The linear functional I in Eq. (1) is defined with respect to the origin of correlator space, and we adopt the minimization convention. With this choice, any genuine quantum violation implies $\beta_Q/\beta_C > 1$, reflecting that in the primal space the quantum set strictly contains the local polytope; our method also works in the maximization convention [20]. In addition, the functional can also be referenced to other points, e.g. $I = \sum_{\boldsymbol{\mu}} \alpha_{\boldsymbol{\mu}} (\langle A_{\boldsymbol{\mu}} \rangle - O_{\boldsymbol{\mu}})$. Our method remains applicable as long as the point $O_{\boldsymbol{\mu}}$ lies inside the local polytope, in which case the optimization identifies a nearby facet.

Benchmarking CHSH inequality.—We start with a bipartite scenario in which each party performs two

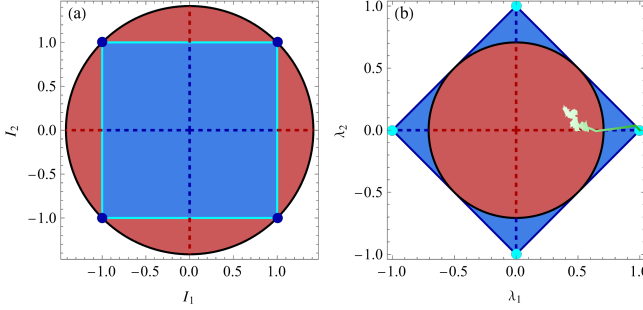


FIG. 1. Illustration of the ratio-optimization procedure for a two-body Bell inequality. The maximum ratio identifies a tight Bell inequality. (a) Local (blue) polytope and quantum (red) convex set in the primal space, projected onto a two-dimensional plane spanned by the linear functionals I_1 and I_2 . Blue dots represent the vertices of the local polytope after projection. (b) Corresponding objects in the dual-space cross-section, where cyan dots represent tight Bell inequalities. In both panels, the dashed curve indicates the tight inequality achieving the largest ratio. The light-green curve shows the projected trajectory of the coefficients α_{kl} during the optimization, plotted in the (λ_1, λ_2) cross-section, demonstrating convergence to a CHSH inequality.

measurements with two possible outcomes. The linear functional is expressed by the correlators as $I = \sum_{k,l=0}^1 \alpha_{kl} \langle A_k B_l \rangle$, where the outcomes of A_k and B_l are ± 1 . For simplicity, we consider the symmetric inequality with $\alpha_{10} = \alpha_{01}$. To evaluate the quantum value, we assign the symmetric measurement setting $\hat{A}_0 = \hat{\sigma}_z^A$, $\hat{B}_0 = \hat{\sigma}_z^B$, $\hat{A}_1 = \cos \theta \hat{\sigma}_z^A + \sin \theta \hat{\sigma}_x^A$, $\hat{B}_1 = \cos \theta \hat{\sigma}_z^B + \sin \theta \hat{\sigma}_x^B$ and obtain the Bell operator $\hat{I}(\theta)$.

Figure 1(a) shows a two-dimensional affine projection of the local polytope and the quantum convex set in the primal space of correlators, using the two linear functionals $I_1 = (\langle A_0 B_0 \rangle + \langle A_0 B_1 \rangle + \langle A_1 B_0 \rangle - \langle A_1 B_1 \rangle)/2$ and $I_2 = (-\langle A_0 B_0 \rangle + \langle A_0 B_1 \rangle + \langle A_1 B_0 \rangle + \langle A_1 B_1 \rangle)/2$ [37, 41, 42]. Figure 1(b) shows the corresponding dual-space cross-section (the space of Bell functionals up to scale). In general, dual extreme points are represented by coefficients $\lambda_{\mu} = \alpha_{\mu}/\beta$, so that the inequality reads $\sum_{\mu} \lambda_{\mu} \langle A_{\mu} \rangle \geq -1$. Facet Bell inequalities correspond to vertices of the dual polytope at $\beta = \beta_C$; the dual quantum boundary is obtained at $\beta = \beta_Q$. We evaluate β_C and β_Q for the family $I = \lambda_1 I_1 + \lambda_2 I_2$ spanned by I_1 and I_2 . In the dual space, the admissible region is the set of (λ_1, λ_2) such that every point in the primal space satisfies $\lambda_1 I_1 + \lambda_2 I_2 \geq -1$.

We then apply our gradient-based optimization to the coefficients α_{kl} . The light-green curve shows the optimization trajectory (projected onto the dual cross-section), which converges to the CHSH facet, attaining the maximum ratio $\Delta^{\max} = \sqrt{2}$ ($\beta_Q = -2\sqrt{2}$ vs. $\beta_C = -2$). The initial linear functional is $I = 0.3\langle A_0 B_1 \rangle + 0.3\langle A_1 B_0 \rangle - 0.5\langle A_1 B_1 \rangle$, where the gradient

vanishes; to escape this flat region we add small random perturbations to the coefficients α_{μ} [40].

Permutation-invariant Bell inequalities.—Now we focus on PI Bell inequalities involving up to two-body correlators. For the $(N, m, 2)$ scenario, the linear functional takes the form $I = \sum_{k=0}^{m-1} \alpha_k \langle S_k \rangle + \sum_{k,l=0}^{m-1} \alpha_{kl} \langle S_{kl} \rangle / 2$, with one- and two-body observables $S_k := \sum_{i=1}^N A_k^{(i)}$ and $S_{kl} := \sum_{i \neq j} A_k^{(i)} A_l^{(j)}$, where $(i), (j)$ label the sites and k, l denote the measurement. Using $S_{kl} = \{S_k, S_l\}/2 - Z_{kl}$, with $Z_{kl} := \sum_{i=1}^N (A_k^{(i)} A_l^{(i)} + A_l^{(i)} A_k^{(i)})/2$ [27, 40], we formally rewrite the linear functional I as

$$I = \sum_{k=0}^{m-1} \alpha_k \langle S_k \rangle + \frac{1}{2} \sum_{k,l=0}^{m-1} \alpha_{kl} \langle S_k S_l - Z_{kl} \rangle, \quad (5)$$

under the constraint $-N + |\langle S_k \rangle + \langle S_l \rangle| \leq \langle Z_{kl} \rangle \leq N - |\langle S_k \rangle - \langle S_l \rangle|$. To evaluate the classical bound β_C , we consider the local deterministic strategies for S_k and Z_{kl} . It is known that vertices of the local polytope are characterized by $S_k \in \{-N, -N+2, \dots, N-2, N\}$ and $Z_{kl} = -N + |S_k + S_l|$ or $N - |S_k - S_l|$ according to the sign of α_{kl} [27, 40]. For the quantum value, we adopt the symmetric measurement setting with the observables $\hat{S}_k = 2 \cos \theta_k \hat{S}_z + 2 \sin \theta_k \hat{S}_x$ and $\hat{Z}_{kl} = N \cos(\theta_k - \theta_l)$, where \hat{S}_x and \hat{S}_z are the collective spin operators [27]. Restricting the measurements on qubits and onto the real circle of the Bloch sphere is sufficient to attain the maximum quantum violation for $m = 2$ by virtue of Jordan's lemma [43]. The quantum value is obtained as the variational minimum of the ground-state energy of the Hamiltonian $\hat{I}(\theta)$ over different measurement settings $\theta = \{\theta_k\}_k$.

We apply our gradient-based optimization to the $(N, 2, 2)$ scenario [27]. For finite N , we seek the coefficients $\alpha_{\mu} = (\alpha_0, \alpha_1, \alpha_{00}, \alpha_{01}, \alpha_{11})$ that maximize the ratio $\Delta_{N,2}$ and we denote the global maximum ratio for given N as $\Delta_{N,2}^{\max}$. The vertices of the local polytope are the extreme points of the five-dimensional space spanned by $\langle S_{\mu} \rangle = (\langle S_0 \rangle, \langle S_1 \rangle, \langle S_{00} \rangle, \langle S_{01} \rangle, \langle S_{11} \rangle)$. In this scenario, the numerical results show that the Bell inequalities become tight when the ratio attains a local maximum. Therefore, optimization of the coefficients can be used to find tight Bell inequalities (see Table I).

We find a family of tight Bell inequalities related to the coefficients

$$\alpha_{\mu} = \alpha_{1,\mu} + n \alpha_{2,\mu}, \quad (6)$$

with $\alpha_{1,\mu} = (1, -1, 1, 1, 1)$ and $\alpha_{2,\mu} = (1, 1, 0, 0, 0)$ and $n \in \{-2N + 7, -2N + 9, \dots, 2N - 9, 2N - 7\}$. The maximum ratio is reached by $n = \pm 1$. Figure 2(a) and (b) show the affine projection and the cross section for this family of tight Bell inequalities for the $(12, 2, 2)$ scenario, respectively. The cyan dots represent the vertices of the local polytope. The blue and red dashed lines

show the classical bound and the quantum value, respectively. This family includes the Bell inequality with coefficients $(2, 0, 1, 1, 1)$ which achieves the largest ratio as N increases.

TABLE I: Maximum ratio $\Delta_{N,2}^{\max}$, classical bound β_C , and corresponding coefficients for the $(N, 2, 2)$ scenario.

| N | $\Delta_{N,2}^{\max}$ | β_C | α_{μ} |
|-----|-----------------------|-----------|----------------------|
| 2 | $\sqrt{2}$ | -2 | $(0, 0, 1, 1, -1)$ |
| 3 | 1.11303 | -18 | $(6, 2, 6, 3, -2)$ |
| 4 | 1.11302 | -18 | $(0, 0, 6, 2, -1)$ |
| 5 | 1.05904 | -80 | $(20, 4, 20, 5, -2)$ |
| 6 | 1.05884 | -60 | $(0, 0, 15, 3, -1)$ |
| 7 | 1.03384 | -14 | $(2, 0, 1, 1, 1)$ |
| 8 | 1.04058 | -16 | $(2, 0, 1, 1, 1)$ |
| 10 | 1.05528 | -20 | $(2, 0, 1, 1, 1)$ |
| 20 | 1.09814 | -40 | $(2, 0, 1, 1, 1)$ |
| 40 | 1.13479 | -80 | $(2, 0, 1, 1, 1)$ |

We now apply our method to the $(N, 3, 2)$ scenario. Since adding a third measurement setting increases the achievable ratio, $\Delta_{N,3}^{\max} \geq \Delta_{N,2}^{\max}$, the corresponding inequalities are more robust and easier to certify experimentally. For $m = 3$, all tight Bell inequalities can be enumerated only when $N < 5$ [44], and we list these inequalities in [40]. For larger N , a complete enumeration is infeasible, but our gradient-based method remains applicable for searching facet Bell inequalities. We find $\Delta_{N,3}^{\max} = \Delta_{N,2}^{\max}$ for small N , while for $N \geq 4$ three measurements yield a strictly larger ratio, $\Delta_{N,3}^{\max} > \Delta_{N,2}^{\max}$.

We find a family of tight Bell inequalities whose coefficients are given by Eq. (6) with $\alpha_{1,\mu} = (2, 0, -2, 1, 1, 1, 1, 1, 1)$ and $\alpha_{2,\mu} = (1, 1, 1, 0, 0, 0, 0, 0, 0)$, and $n \in \{-2N+1, -2N+3, \dots, 2N-3, 2N-1\}$ for even N and $n \in \{-2N, -2N+2, \dots, 2N-2, 2N\}$ for odd N , where $\alpha_{1,\mu}$ corresponds to the Bell inequality considered in Ref. [45]. Figure 2(c) and (d) show the affine projection and the cross section of this family for $N = 11$, respectively. Interestingly, we find that for sufficiently large N the optimal Bell inequality with largest ratio does not belong to this family. For example, for $N = 141$, we find $\alpha_{\mu} = (694, 0, -694, 385, 309, 385, 248, 309, 385)$ with a ratio $\Delta = 1.21485$, which exceeds the ratio $\Delta = 1.21482$ of $\alpha_{1,\mu}$. This implies that with more measurements, finding the Bell inequality with the largest ratio is no longer as straightforward as for $m = 2$. Nevertheless, our gradient-based method remains effective in identifying inequalities with larger ratios (see Table II).

TABLE II: Selected tight Bell inequalities for $m = 3$ with their ratios and classical bounds. These inequalities are distinct from those in the $m = 2$ scenario.

| N | $\Delta_{N,3}$ | β_C | α_{μ} |
|-----|----------------|-----------|---------------------------------|
| 2 | $5/4$ | -8 | $(2, 1, 1, 2, 2, 2, -2, 1, -2)$ |

(continued on next page)

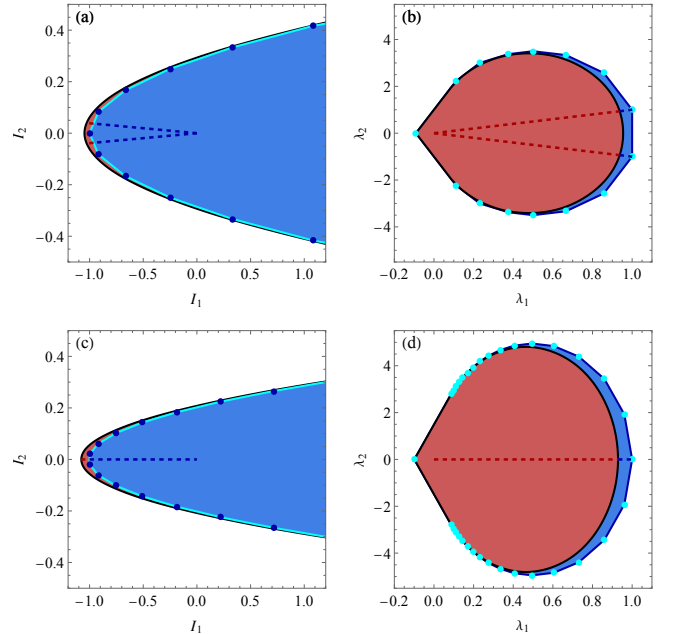


FIG. 2. Two-dimensional affine projections (left) and corresponding cross-sections (right) for the $(N, m, 2)$ scenarios. (a) and (b) $N = 12, m = 2$. The projection plane is spanned by the two functionals with coefficients $\alpha_{1,\mu} = (1, -1, 1, 1, 1)/24$ and $\alpha_{2,\mu} = (1, 1, 0, 0, 0)/24$. (c) and (d) $N = 11, m = 3$. The affine projection is spanned by $\alpha_{1,\mu} = (2, 0, -2, 1, 1, 1, 1, 1)/49$ and $\alpha_{2,\mu} = (1, 1, 1, 0, 0, 0, 0, 0)/49$. Dashed lines indicate the maximum ratio in the affine projections and cross sections. Blue dots (left panels) show the vertices in the primal affine projections and correspond to blue lines (right panels) in the dual cross-sections. Cyan lines (left panels) denote tight Bell facets, which map to cyan vertices (right panels).

(continued from previous page)

| N | $\Delta_{N,3}$ | β_C | α_{μ} |
|-----|----------------|-----------|---|
| 3 | 1.10033 | -42 | $(6, 6, 4, 6, 6, 3, 0, 3, -4)$ |
| 4 | 1.11760 | -30 | $(0, 0, 0, 3, 3, 2, 3, 0, -1)$ |
| 5 | 1.00538 | -56 | $(10, 4, 0, 3, 3, 2, 3, 2, 1)$ |
| 6 | 1.06750 | -150 | $(0, 0, 0, 15, 10, 5, 5, 1, -2)$ |
| 7 | 1.02686 | -113 | $(8, 6, 0, 5, -4, 4, 3, -3, 3)$ |
| 8 | 1.04123 | -120 | $(7, 7, 0, 4, -4, 3, 4, -3, 2)$ |
| 10 | 1.06249 | -360 | $(25, 8, 7, 10, -9, 8, 8, -7, 6)$ |
| 20 | 1.11557 | -840 | $(19, 19, 0, 10, -10, 9, 10, -9, 8)$ |
| 40 | 1.15932 | -3480 | $(39, 39, 0, 20, -20, 19, 20, -19, 18)$ |

Optimization in the thermodynamic limit $N \rightarrow \infty$.— Permutation symmetry admits a rigorous mean-field solution in the thermodynamic limit. We introduce continuous variables $s_k = \langle \mathcal{S}_k \rangle / N$ and $z_{kl} = \langle \mathcal{Z}_{kl} \rangle / N$, so that the state concentrates on certain s_k and z_{kl} with the two-body correlator approaching $\langle \mathcal{S}_k \mathcal{S}_l \rangle = N^2 s_k s_l$. Equation (5) then becomes $I = N^2 \sum_{k,l=0}^{m-1} \alpha_{kl} s_k s_l / 2 + N \sum_{k=0}^{m-1} \alpha_k s_k - N \sum_{k,l=0}^{m-1} \alpha_{kl} z_{kl} / 2$, where the first term

scales as N^2 and the others as N . For the classical case, the local polytope is $\mathcal{N}_C = \{(\mathbf{s}, \mathbf{z}) \mid -1 \leq s_k \leq 1, z_{kk} = 1, -1 \leq z_{kl} \leq 1, -1 + |s_k + s_l| \leq z_{kl} \leq 1 - |s_k - s_l|\}$, with $\mathbf{s} = \{s_k\}_{k=0}^{m-1}$ and $\mathbf{z} = \{z_{kl}\}_{k,l=0}^{m-1}$. For the quantum case, we find the convex set is given by $\mathcal{N}_Q = \{(\mathbf{s}, \mathbf{z}) \mid z_{kk} = 1, z_{kl}^2 + s_k^2 + s_l^2 - 2z_{kl}s_k s_l \leq 1\}$. The classical bound and the minimal quantum value in the thermodynamic limit can be written as the optimization over the two sets.

The ratios in the $N \rightarrow \infty$ limit are summarized in Table III. We consider two optimizations: (i) fixing all $\alpha_{kl} = 1$ and optimizing only the single-body coefficients α_k ; (ii) optimizing both α_{kl} and α_k , which yields larger ratios for finite m . The large m admits the same results $\Delta_{\infty, \infty} = \coth(1) \approx 1.31304$. The detailed derivations is left in [40].

TABLE III: Ratios for the scenario $(N, m, 2)$ in the limit $N \rightarrow \infty$. The second column shows $\Delta_{\infty, m}$ with fixed $\alpha_{kl} = 1$ (only α_k optimized), and the third column shows the maximum ratio $\Delta_{\infty, m}^{\max}$ when both α_{kl} and α_k are optimized.

| m | $\Delta_{\infty, m}$ | $\Delta_{\infty, m}^{\max}$ |
|----------|----------------------|-----------------------------|
| 2 | $5/4$ | $5/4$ |
| 3 | 1.28458 | $9/7$ |
| 4 | 1.29711 | $353/272$ |
| 5 | 1.30285 | $275/211$ |
| 6 | 1.30597 | $66637/51012$ |
| ∞ | $\coth(1)$ | $\coth(1)$ |

Conclusion.—We proposed a gradient-based method for optimizing Bell inequalities, applied it to PI Bell inequalities involving up to two-body dichotomic correlators, and identified new tight Bell inequalities for the scenario of three measurements per party ($m = 3$). We also derive analytical expressions for the maximum ratio in the thermodynamic limit $N \rightarrow \infty$, which yield simple integer ratios for small m and converge to $\coth(1)$ in the joint limit $N, m \rightarrow \infty$.

The framework is general and naturally extends to certifying quantumness in many-body systems [18–20, 46]. In particular, one can fix a Bell operator and inversely optimize the classical bound, leading to a more robust certification of nonlocality for the given quantum state [20, 47]. It can also be adapted to PI Bell inequalities involving higher-body correlators [30], translationally invariant Bell inequalities [28, 48–52], and other more general Bell inequalities [33, 53–56]. Here we determine the quantum value as the ground-state energy of its corresponding Hamiltonian within the symmetric measurement setting, providing a variational upper bound at fixed Hilbert-space dimension. A certified lower bound can be established through SDP-based relaxation methods [57–59], which we leave for future work.

Acknowledgments.—We thank Owidiusz Makuta and Eloïc Vallée for reading the manuscript and offering helpful comments. J.F.C., M.H., and J.T. acknowledge the

support received from the European Union’s Horizon Europe research and innovation programme through the ERC StG FINE-TEA-SQUAD (Grant No. 101040729). This publication is part of the ‘Quantum Inspire - the Dutch Quantum Computer in the Cloud’ project (with project number [NWA.1292.19.194]) of the NWA research program ‘Research on Routes by Consortia (ORC)’, which is funded by the Netherlands Organization for Scientific Research (NWO). Parts of this work were performed by using the compute resources from the Academic Leiden Interdisciplinary Cluster Environment (ALICE) provided by Leiden University. The views and opinions expressed here are solely those of the authors and do not necessarily reflect those of the funding institutions. Neither of the funding institutions can be held responsible for them.

* jinfuchen@lorentz.leidenuniv.nl

† mengyao@lorentz.leidenuniv.nl

‡ tura@lorentz.leidenuniv.nl

- [1] A. Einstein, B. Podolsky, and N. Rosen, Physical Review **47**, 777 (1935).
- [2] J. S. Bell, Physics Physique Fizika **1**, 195 (1964).
- [3] J. F. Clauser, M. A. Horne, A. Shimony, and R. A. Holt, Physical Review Letters **23**, 880 (1969).
- [4] L. J. Landau, Foundations of Physics **18**, 449 (1988).
- [5] L. Masanes, Necessary and sufficient condition for quantum-generated correlations (2003), arXiv:quant-ph/0309137.
- [6] B. Hensen, H. Bernien, A. E. Dréau, A. Reiserer, N. Kalb, M. S. Blok, J. Ruitenberg, R. F. L. Vermeulen, R. N. Schouten, C. Abellán, W. Amaya, V. Pruneri, M. W. Mitchell, M. Markham, D. J. Twitchen, D. Elkouss, S. Wehner, T. H. Taminiau, and R. Hanson, Nature **526**, 682 (2015).
- [7] M. Giustina, M. A. M. Versteegh, S. Wengerowsky, J. Handsteiner, A. Hochrainer, K. Phelan, F. Steinlechner, J. Kofler, J.-A. Larsson, C. Abellán, W. Amaya, V. Pruneri, M. W. Mitchell, J. Beyer, T. Gerrits, A. E. Lita, L. K. Shalm, S. W. Nam, T. Scheidl, R. Ursin, B. Wittmann, and A. Zeilinger, Physical Review Letters **115**, 250401 (2015).
- [8] L. K. Shalm, E. Meyer-Scott, B. G. Christensen, P. Bierhorst, M. A. Wayne, M. J. Stevens, T. Gerrits, S. Glancy, D. R. Hamel, M. S. Allman, K. J. Coakley, S. D. Dyer, C. Hodge, A. E. Lita, V. B. Verma, C. Lambrocco, E. Tortorici, A. L. Migdall, Y. Zhang, D. R. Kumor, W. H. Farr, F. Marsili, M. D. Shaw, J. A. Stern, C. Abellán, W. Amaya, V. Pruneri, T. Jennewein, M. W. Mitchell, P. G. Kwiat, J. C. Bienfang, R. P. Mirin, E. Knill, and S. W. Nam, Physical Review Letters **115**, 250402 (2015).
- [9] W. Rosenfeld, D. Burchardt, R. Garthoff, K. Redeker, N. Ortegel, M. Rau, and H. Weinfurter, Physical Review Letters **119**, 010402 (2017).
- [10] S. Storz, J. Schär, A. Kulikov, P. Magnard, P. Kurpiers, J. Lütolf, T. Walter, A. Copetudo, K. Reuer, A. Akin, J.-C. Besse, M. Gabureac, G. J. Norris, A. Rosario, F. Marul

tin, J. Martinez, W. Amaya, M. W. Mitchell, C. Abellán, J.-D. Bancal, N. Sangouard, B. Royer, A. Blais, and A. Wallraff, *Nature* **617**, 265 (2023).

[11] A. Acín, N. Brunner, N. Gisin, S. Massar, S. Pironio, and V. Scarani, *Physical Review Letters* **98**, 230501 (2007).

[12] S. Pironio, A. Acín, N. Brunner, N. Gisin, S. Massar, and V. Scarani, *New Journal of Physics* **11**, 045021 (2009).

[13] U. Vazirani and T. Vidick, *Physical Review Letters* **113**, 140501 (2014).

[14] F. Xu, X. Ma, Q. Zhang, H.-K. Lo, and J.-W. Pan, *Reviews of Modern Physics* **92**, 025002 (2020).

[15] S. Pironio, A. Acín, S. Massar, A. B. De La Giroday, D. N. Matsukevich, P. Maunz, S. Olmschenk, D. Hayes, L. Luo, T. A. Manning, and C. Monroe, *Nature* **464**, 1021 (2010).

[16] A. Fyrillas, B. Bourdoncle, A. Maños, P.-E. Emeriau, K. Start, N. Margaria, M. Morassi, A. Lemaître, I. Sagnes, P. Stepanov, T. H. Au, S. Boissier, N. Somaschi, N. Maring, N. Belabas, and S. Mansfield, *PRX Quantum* **5**, 020348 (2024).

[17] C. Zhang, Y. Li, X.-M. Hu, Y. Xiang, C.-F. Li, G.-C. Guo, J. Tura, Q. Gong, Q. He, and B.-H. Liu, *Physical Review Letters* **134**, 090201 (2025).

[18] I. Šupić and J. Bowles, *Quantum* **4**, 337 (2020).

[19] Y. Li, Y. Xiang, J. Tura, and Q. He, *Physical Review Letters* **135**, 060201 (2025).

[20] F. Baccari, R. Augusiak, I. Šupić, J. Tura, and A. Acín, *Physical Review Letters* **124**, 020402 (2020).

[21] B. Chazelle, *Discrete & Computational Geometry* **10**, 377 (1993).

[22] I. Pitowsky, *Quantum Probability — Quantum Logic*, Lecture Notes in Physics, Vol. 321 (Springer-Verlag, Berlin/Heidelberg, 1989).

[23] I. Pitowsky, *Mathematical Programming* **50**, 395 (1991), publisher: Springer.

[24] J.-D. Bancal, N. Brunner, N. Gisin, and Y.-C. Liang, *Physical Review Letters* **106**, 020405 (2011).

[25] M. Froissart, *Il Nuovo Cimento B* **64**, 241 (1981).

[26] I. Pitowsky and K. Svozil, *Physical Review A* **64**, 014102 (2001).

[27] J. Tura, R. Augusiak, A. B. Sainz, T. Vértesi, M. Lewenstein, and A. Acín, *Science* **344**, 1256 (2014).

[28] Z. Wang, S. Singh, and M. Navascués, *Physical Review Letters* **118**, 230401 (2017).

[29] R. Schmied, J.-D. Bancal, B. Allard, M. Fadel, V. Scarani, P. Treutlein, and N. Sangouard, *Science* **352**, 441 (2016).

[30] J. Guo, J. Tura, Q. He, and M. Fadel, *Physical Review Letters* **131**, 070201 (2023).

[31] C. Marconi, G. Müller-Rigat, J. Romero-Pallejà, J. Tura, and A. Sanpera, *Symmetric quantum states: a review of recent progress* (2025), arXiv:2506.10185 [quant-ph].

[32] J. Wang, S. Paesani, Y. Ding, R. Santagati, P. Skrzypczyk, A. Salavrakos, J. Tura, R. Augusiak, L. Mančinska, D. Bacco, D. Bonneau, J. W. Silverstone, Q. Gong, A. Acín, K. Rottwitt, L. K. Oxenløwe, J. L. O'Brien, A. Laing, and M. G. Thompson, *Science* **360**, 285 (2018).

[33] K. Wang, W. Li, S. Xu, M. Hu, J. Chen, Y. Wu, C. Zhang, F. Jin, X. Zhu, Y. Gao, Z. Tan, Z. Cui, A. Zhang, N. Wang, Y. Zou, T. Li, F. Shen, J. Zhong, Z. Bao, Z. Zhu, Z. Song, J. Deng, H. Dong, X. Zhang, P. Zhang, W. Jiang, Z. Lu, Z.-Z. Sun, H. Li, Q. Guo, Z. Wang, P. Emonts, J. Tura, C. Song, H. Wang, and D.-L. Deng, *Physical Review X* **15**, 021024 (2025).

[34] S. Gómez, D. Uzcátegui, I. Machuca, E. S. Gómez, S. P. Walborn, G. Lima, and D. Goyeneche, *Scientific Reports* **11**, 20489 (2021).

[35] W. Li, M. Hu, K. Wang, S. Xu, Z. Lu, J. Chen, Y. Wu, C. Zhang, F. Jin, X. Zhu, Y. Gao, Z. Cui, A. Zhang, N. Wang, Y. Zou, F. Shen, J. Zhong, Z. Bao, Z. Zhu, P. Zhang, H. Li, Q. Guo, Z. Wang, D.-L. Deng, C. Song, H. Wang, P. Emonts, and J. Tura, *Improved Nonlocality Certification via Bouncing between Bell Operators and Inequalities* (2024), arXiv:2407.12347 [quant-ph].

[36] D.-L. Deng, *Physical Review Letters* **120**, 240402 (2018).

[37] N. Brunner, D. Cavalcanti, S. Pironio, V. Scarani, and S. Wehner, *Reviews of Modern Physics* **86**, 419 (2014).

[38] M. Fadel and J. Tura, *Quantum* **2**, 107 (2018).

[39] Z. Wang and M. Navascués, *Proceedings of the Royal Society A: Mathematical, Physical and Engineering Sciences* **474**, 20170822 (2018).

[40] Supplemental Material.

[41] C. Branciard, *Physical Review A* **83**, 032123 (2011).

[42] K. T. Goh, J. Kaniewski, E. Wolfe, T. Vértesi, X. Wu, Y. Cai, Y.-C. Liang, and V. Scarani, *Physical Review A* **97**, 022104 (2018).

[43] B. Toner and F. Verstraete, *Monogamy of Bell correlations and Tsirelson's bound* (2006), arXiv:quant-ph/0611001.

[44] K. Fukuda, *Cddlib reference manual* (2003).

[45] S. Wagner, R. Schmied, M. Fadel, P. Treutlein, N. Sangouard, and J.-D. Bancal, *Physical Review Letters* **119**, 170403 (2017).

[46] A. Tavakoli, A. Pozas-Kerstjens, M.-X. Luo, and M.-O. Renou, *Reports on Progress in Physics* **85**, 056001 (2022).

[47] O. Gühne, G. Tóth, P. Hyllus, and H. J. Briegel, *Physical Review Letters* **95**, 120405 (2005).

[48] J. Tura, G. De Las Cuevas, R. Augusiak, M. Lewenstein, A. Acín, and J. Cirac, *Physical Review X* **7**, 021005 (2017).

[49] M. Hu and J. Tura, *Tropical contraction of tensor networks as a Bell inequality optimization toolset* (2024), arXiv:2208.02798 [quant-ph].

[50] M. Hu, E. Vallée, T. Seynnaeve, P. Emonts, and J. Tura, *Characterizing Translation-Invariant Bell Inequalities using Tropical Algebra and Graph Polytopes* (2024), arXiv:2407.08783 [quant-ph].

[51] J. Tura, A. B Sainz, T. Vértesi, A. Acín, M. Lewenstein, and R. Augusiak, *Journal of Physics A: Mathematical and Theoretical* **47**, 424024 (2014).

[52] P. Emonts, M. Hu, A. Aloy, and J. Tura, *Physical Review A* **110**, 032201 (2024).

[53] C. Śliwa, *Physics Letters A* **317**, 165 (2003).

[54] S. López-Rosa, Z.-P. Xu, and A. Cabello, *Physical Review A* **94**, 062121 (2016).

[55] F. Bernards and O. Gühne, *Physical Review A* **104**, 012206 (2021).

[56] F. Bernards and O. Gühne, *Physical Review Letters* **125**, 200401 (2020).

[57] M. Fadel and J. Tura, *Physical Review Letters* **119**, 230402 (2017).

[58] M. Navascués, S. Pironio, and A. Acín, *New Journal of Physics* **10**, 073013 (2008).

[59] A. Tavakoli, A. Pozas-Kerstjens, P. Brown, and M. Araújo, *Reviews of Modern Physics* **96**, 045006 (2024).

Supplemental Material: Optimizing quantum violation for multipartite facet Bell inequalities

Jin-Fu Chen (陈劲夫) ^{1, 2, *} Mengyao Hu (胡梦瑶) ^{1, 2, †} and Jordi Tura ^{1, 2, ‡}

¹*Instituut-Lorentz, Universiteit Leiden, P.O. Box 9506, 2300 RA Leiden, The Netherlands*

² *$\langle aQa^L \rangle$ Applied Quantum Algorithms, Universiteit Leiden, The Netherlands*

(Dated: January 21, 2026)

The supplementary material is devoted to providing detailed derivations in the main text. In Section I, we show that the ratio between the quantum value and the classical bound of Bell inequalities achieves a local maximum when the inequalities are tight. In Section II, we introduce the basics of permutation-invariant (PI) Bell inequalities for the $(N, m, 2)$ scenario with upto two-body correlators, where each of the N parties performs one of the m possible measurements with binary outcomes ± 1 . In Section III, we introduce a gradient-based method that optimizes the coefficients of Bell inequalities to achieve the maximum ratio. We show explicit results for Clauser-Horne-Shimony-Holt (CHSH) inequalities in Section IV, and for PI Bell Inequalities with $m = 2$ and $m = 3$ in Section V. Analytical results for PI Bell Inequalities in the thermodynamic limit $N \rightarrow \infty$ are given in Section VI.

I. ILLUSTRATION FOR TIGHT BELL INEQUALITIES AS LOCAL MAXIMA OF THE RATIO

The numerical results (Tables I and II in the main text) show that the tight Bell inequality corresponds to a local maximum of the quantum-to-classical ratio $\Delta := \beta_Q / \beta_C$. Here we interpret this observation from the geometric point of view.

In the primal space, we consider a two-dimensional affine projection, as shown in Fig. S1, spanned by tight Bell inequalities. The facet (cyan) appears as an edge of the polygon. When the optimal quantum point (red) is unique, the ratio attains a strict local maximum at the tight Bell inequality, as shown in Fig. S1(a), for example, the CHSH inequality. In contrast, as shown in Fig. S1(b), two facet Bell inequalities (cyan) attain their maximum at the same quantum point (red dot) for example, the two Bell inequalities $\alpha_{1,\mu} = (0, 0, 0, 6, 3, 3, 0, 1, -2)$ and $\alpha_{2,\mu} = (0, 0, 0, 0, 3, 1, 6, 3, -2)$ in the $(4, 3, 2)$ scenario. Consequently, the ratio remains constant for any convex combination of these two inequalities, and the first derivatives with respect to the coefficients α_μ vanish. Figure S1(c) shows trivial facets with the ratio $\Delta = 1$, for example, the two Bell inequalities $\alpha_{1,\mu} = (1, 0, 1, 0, 0, 0)$ and $\alpha_{2,\mu} = (0, 1, 0, 0, 1)$ in the $(2, 2, 2)$ scenario.

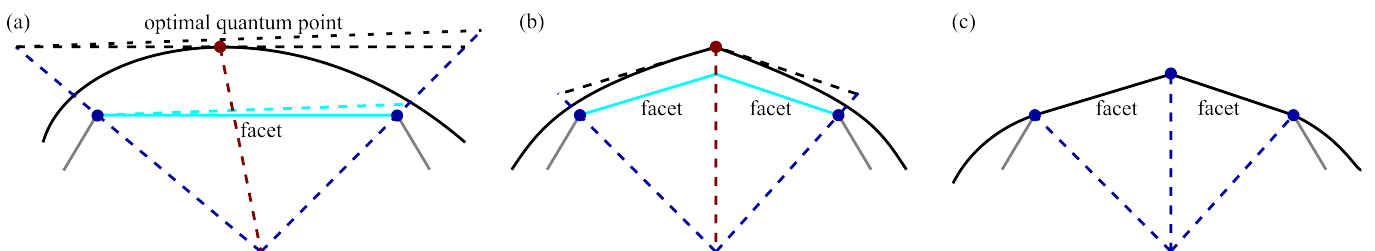


FIG. S1. Illustration of a tight Bell inequality with a local maximum of the ratio. Here we show a two-dimensional affine projection in the primal space of the correlators. (a) For the tight Bell inequality (cyan line), there exists a unique optimal quantum point (red dot), which guarantees that the ratio has a strict local maximum. (b) Two facet Bell inequalities (cyan lines) share the same optimal quantum point (red dot). Consequently, the ratio is fixed for any convex combination of these two inequalities. (c) Two facets corresponding to trivial Bell inequalities that do not separate the quantum set from the local polytope.

* jinfuchen@lorentz.leidenuniv.nl

† mengyao@lorentz.leidenuniv.nl

‡ tura@lorentz.leidenuniv.nl

II. PERMUTATION-INVARIANT BELL INEQUALITIES FOR $(N, m, 2)$ SCENARIO

To explore the Bell nonlocality in a larger and more complex systems, it is essential to study multipartite Bell inequalities. We consider the $(N, m, 2)$ Bell scenario, where N spatially separated parties share an N -partite resource. Each party can choose one of m measurements, each yielding two outcomes. We will apply the method of maximizing the ratio between the quantum value and the classical bound for PI Bell inequalities with upto two-body correlators in the $(N, m, 2)$ scenario.

A PI Bell inequality with upto two body correlators is given by

$$I = \sum_{k=0}^{m-1} \alpha_k \langle \mathcal{S}_k \rangle + \frac{1}{2} \sum_{k,l=0}^{m-1} \alpha_{kl} \langle \mathcal{S}_{kl} \rangle \quad (\text{S1})$$

$$= \sum_{k=0}^{m-1} \alpha_k \langle \mathcal{S}_k \rangle + \frac{1}{2} \sum_{k,l=0}^{m-1} \alpha_{kl} \langle \mathcal{S}_k \mathcal{S}_l - \mathcal{Z}_{kl} \rangle \geq \beta_C, \quad (\text{S2})$$

where the one-body and two-body observables are collected into $\mathcal{S}_k := \sum_{i=1}^N A_k^{(i)}$ and $\mathcal{S}_{kl} := \sum_{i \neq j} A_k^{(i)} A_l^{(j)} = \mathcal{S}_k \mathcal{S}_l - \mathcal{Z}_{kl}$ with $\mathcal{Z}_{kl} := \sum_{i=1}^N (A_k^{(i)} A_l^{(i)} + A_l^{(i)} A_k^{(i)})/2$. We note that in the equality $ab = 1 - |a - b| = -1 + |a + b|$ holds for any $a, b = \pm 1$. For the classical case we obtain

$$\mathcal{Z}_{kl} = N - \sum_{i=1}^N |A_k^{(i)} - A_l^{(i)}| \quad (\text{S3})$$

$$= -N + \sum_{i=1}^N |A_k^{(i)} + A_l^{(i)}|. \quad (\text{S4})$$

Applying the triangle inequality to Eqs (S3) and (S4), one finds that $\langle \mathcal{Z}_{kl} \rangle$ is restricted inside a regular tetrahedron [S1]

$$-N + |\langle \mathcal{S}_k \rangle + \langle \mathcal{S}_l \rangle| \leq \langle \mathcal{Z}_{kl} \rangle \leq N - |\langle \mathcal{S}_k \rangle - \langle \mathcal{S}_l \rangle|. \quad (\text{S5})$$

The classical bound β_C is given by the local deterministic strategies corresponding to the vertices of the local polytope \mathcal{L} in the correlator space. Since the observables have fixed outcomes in the deterministic strategies, the expectation brackets $\langle \cdot \rangle$ are omitted in the enumeration of vertices. For the vertices, \mathcal{S}_k and \mathcal{Z}_{kl} take integer values with the same parity as N . Since I depends linearly on \mathcal{Z}_{kl} , it attains extreme values under the constraint (S5). Therefore, evaluating the classical bound $\beta_C := \min_{\langle \mathcal{S}_k \rangle, \langle \mathcal{Z}_{kl} \rangle \in \mathcal{L}} I$ requires considering only extreme points on the surfaces of regular tetrahedrons defined by $(\mathcal{S}_k, \mathcal{S}_l, \mathcal{Z}_{kl})$.

For the quantum case, we adopt the symmetric measurement setting

$$\hat{A}_k^{(i)} = \cos \theta_k \hat{\sigma}_z^{(i)} + \sin \theta_k \hat{\sigma}_x^{(i)}, \quad (\text{S6})$$

where $\hat{\sigma}_z^{(i)}$ and $\hat{\sigma}_x^{(i)}$ are Pauli operators of site i . The observables $\hat{\mathcal{S}}_k = \sum_{i=1}^N \hat{A}_k^{(i)}$ can be represented by the collective spin operators

$$\hat{\mathcal{S}}_k = 2 \cos \theta_k \hat{S}_z + 2 \sin \theta_k \hat{S}_x, \quad (\text{S7})$$

where \hat{S}_x , \hat{S}_y , and \hat{S}_z are the collective spin operators. In the \hat{S}_z eigenbasis $|m\rangle : m = N/2, N/2 - 1, \dots, -N/2 + 1, -N/2$, these matrices are given by

$$(\hat{S}_z)_{m,m'} = m \delta_{m,m'}, \quad (\text{S8})$$

$$(\hat{S}_x)_{m,m'} = \frac{1}{2} \left[\sqrt{\left(\frac{N}{2} - m'\right) \left(\frac{N}{2} + m' + 1\right)} \delta_{m,m'+1} + \sqrt{\left(\frac{N}{2} + m'\right) \left(\frac{N}{2} - m' + 1\right)} \delta_{m,m'-1} \right], \quad (\text{S9})$$

$$(\hat{S}_y)_{m,m'} = \frac{1}{2i} \left[\sqrt{\left(\frac{N}{2} - m'\right) \left(\frac{N}{2} + m' + 1\right)} \delta_{m,m'+1} - \sqrt{\left(\frac{N}{2} + m'\right) \left(\frac{N}{2} - m' + 1\right)} \delta_{m,m'-1} \right]. \quad (\text{S10})$$

From Eq. (S7), the operator $\hat{\mathcal{Z}}_{kl}$ is explicitly given by

$$\hat{\mathcal{Z}}_{kl} = N \cos(\theta_k - \theta_l). \quad (\text{S11})$$

Substituting $\hat{\mathcal{S}}_k$ and $\hat{\mathcal{Z}}_{kl}$ into Eq. (S2) gives the Bell operator

$$\hat{I}(\boldsymbol{\theta}) = \sum_{k=0}^{m-1} \alpha_k \hat{\mathcal{S}}_k + \frac{1}{2} \sum_{k,l=0}^{m-1} \alpha_{kl} (\hat{\mathcal{S}}_k \hat{\mathcal{S}}_l - \hat{\mathcal{Z}}_{kl}). \quad (\text{S12})$$

The Bell operator $\hat{I}(\boldsymbol{\theta})$ depends on the coefficients $\alpha_{\boldsymbol{\mu}} = \{\alpha_k, \alpha_{kl}\}_{kl}$, which include both one-body terms α_k and two-body terms α_{kl} , and on the measurement settings $\boldsymbol{\theta} = \{\theta_k\}_k$. For given coefficients $\alpha_{\boldsymbol{\mu}}$, the minimal quantum value $\beta_Q := \min_{|\psi\rangle, \boldsymbol{\theta}} \langle \psi | \hat{I}(\boldsymbol{\theta}) | \psi \rangle = \min_{\boldsymbol{\theta}} \langle \psi^* | \hat{I}(\boldsymbol{\theta}) | \psi^* \rangle$, as the ground-state energy of the Hamiltonian $\hat{I}(\boldsymbol{\theta})$, is obtained by optimizing the measurement angles $\boldsymbol{\theta}$.

III. GRADIENT-BASED METHOD FOR FINDING TIGHT BELL INEQUALITIES

In this section, we present a gradient-based method for optimizing and tightening Bell inequalities. The key idea is to iteratively adjust coefficients in the inequality to minimize the quantum value while keeping the classical bound fixed, progressively incorporating additional vertices of the local polytope until tightness is achieved.

We consider PI Bell inequalities with up to two-body correlators. Starting from the initial coefficients $\alpha_{\boldsymbol{\mu}}$, we consider the set of vertices $\{\mathcal{S}_{\boldsymbol{\mu},j}\}_j$ that saturate the classical bound β_C , where $\boldsymbol{\mu}$ labels the correlators and j indexes the vertices. These vertices $\mathcal{S}_{\boldsymbol{\mu},j}$ satisfy the constraint

$$\sum_{k=0}^{m-1} \alpha_k \mathcal{S}_{k,j} + \frac{1}{2} \sum_{k,l=0}^{m-1} \alpha_{kl} \mathcal{S}_{kl,j} = \beta_C. \quad (\text{S13})$$

If these saturating vertices $\{\mathcal{S}_{\boldsymbol{\mu},j}\}_j$ do not span a full-rank affine space, this equation defines a solution space for the coefficients $\alpha_{\boldsymbol{\mu}}$. Let $M = m(m+3)/2$ be the dimension of the correlator space containing the vectors $\mathcal{S}_{\boldsymbol{\mu}}$. A Bell inequality is tight if and only if the affine hull of its saturating vertices has dimension $M-1$; Otherwise, the inequality is not tight. For example, for $(N, 2, 2)$ scenario, $\mathcal{S}_{\boldsymbol{\mu}} = (\mathcal{S}_0, \mathcal{S}_1, \mathcal{S}_{00}, \mathcal{S}_{01}, \mathcal{S}_{11})$, and $M = 5$.

To explore the solution space of $\alpha_{\boldsymbol{\mu}}$, we arrange all the vertices into a matrix V , which constraint the change of the coefficients as

$$V \delta \alpha_{\boldsymbol{\mu}} = 0. \quad (\text{S14})$$

During the optimization, these constraints [Eq. (S14)] are enforced while maximizing the quantum-to-classical ratio $\Delta = \beta_Q/\beta_C$. Within this constrained space, we perform gradient ascent to increase Δ , updating the coefficients as

$$\delta \alpha_{\boldsymbol{\mu}} = s [I - V^T (VV^T)^+ V] \frac{\partial \Delta}{\partial \alpha_{\boldsymbol{\mu}}}. \quad (\text{S15})$$

Here s is the gradient step size; $\partial \Delta / \partial \alpha_{\boldsymbol{\mu}}$ is the gradient of the ratio; I is the identity matrix; T denotes transpose; the superscript $+$ denotes the Moore-Penrose pseudoinverse [S2, S3]. If the gradient $\partial \Delta / \partial \alpha_{\boldsymbol{\mu}}$ vanishes in the constraint space, we can replace it with random noise for updating $\alpha_{\boldsymbol{\mu}}$.

Our optimization objective is the ratio $\Delta := \beta_Q/\beta_C$, whose derivative with respect to $\alpha_{\boldsymbol{\mu}}$ is generally given by

$$\frac{\partial \Delta}{\partial \alpha_{\boldsymbol{\mu}}} = \frac{1}{\beta_C} \frac{\partial \beta_Q}{\partial \alpha_{\boldsymbol{\mu}}} - \frac{\beta_Q}{\beta_C^2} \frac{\partial \beta_C}{\partial \alpha_{\boldsymbol{\mu}}}. \quad (\text{S16})$$

Both β_Q and β_C vary continuously with $\alpha_{\boldsymbol{\mu}}$, but since the constraint in Eq. (S15) keeps β_C fixed, its derivative with respect to $\alpha_{\boldsymbol{\mu}}$ vanishes within the constraint space. With the Bell operator $\hat{I}(\boldsymbol{\theta})$ in Eq. (S12), the derivative of the quantum value is obtained as

$$\frac{\partial \beta_Q}{\partial \alpha_{\boldsymbol{\mu}}} = \frac{\partial}{\partial \alpha_{\boldsymbol{\mu}}} \min_{\boldsymbol{\theta}, |\psi\rangle} \langle \psi | \hat{I}(\boldsymbol{\theta}) | \psi \rangle \quad (\text{S17})$$

$$= \frac{\partial}{\partial \alpha_{\boldsymbol{\mu}}} \langle \psi^* | \hat{I}(\boldsymbol{\theta}^*) | \psi^* \rangle \quad (\text{S18})$$

$$= \langle \psi^* | \frac{\partial}{\partial \alpha_{\boldsymbol{\mu}}} \hat{I}(\boldsymbol{\theta}^*) | \psi^* \rangle + \frac{\partial \boldsymbol{\theta}^*}{\partial \alpha_{\boldsymbol{\mu}}} \langle \psi^* | \frac{\partial}{\partial \boldsymbol{\theta}} \hat{I}(\boldsymbol{\theta}) \Big|_{\boldsymbol{\theta}=\boldsymbol{\theta}^*} | \psi^* \rangle \quad (\text{S19})$$

$$= \langle \psi^* | \frac{\partial}{\partial \alpha_{\boldsymbol{\mu}}} \hat{I}(\boldsymbol{\theta}^*) | \psi^* \rangle, \quad (\text{S20})$$

where $|\psi^*\rangle$ and $\boldsymbol{\theta}^*$ denote the optimal quantum state and measurement settings. The third equation uses the Feynman–Hellmann theorem since $|\psi^*\rangle$ is the ground state of the Hamiltonian $\hat{I}(\boldsymbol{\theta}^*)$. The fourth equation uses $\langle\psi^*|\partial_{\boldsymbol{\theta}}\hat{I}(\boldsymbol{\theta})|_{\boldsymbol{\theta}=\boldsymbol{\theta}^*}|\psi^*\rangle=0$, since $\boldsymbol{\theta}^*$ minimizes the quantum value.

Once new vertices are identified, they are added to the matrix V , which may increase the rank of V and thereby enlarges the subspace spanned by the current vertex set. We then update the coefficients via the projection operator $I - V^T(VV^T)^+V$ and refine the coefficients $\alpha_{\boldsymbol{\mu}}$ accordingly. A crucial point is the choice of the gradient step size s : it must be selected adaptively and kept sufficiently small, so that the trajectory of the coefficients does not cross into other facet of the polytope. By iterating this cycle of projecting, updating, and incorporating new vertices, the procedure gradually refines the inequality until it becomes tight. For clarity, we summarize the constrained gradient update for Bell inequality coefficients in Algorithm 1. In all the numerical cases, the optimization converges to a facet, except for configurations of the type shown in Figs. S1(b) and S1(c). When the gradient vanishes, introducing random noise in the updates of the coefficients $\alpha_{\boldsymbol{\mu}}$ facilitates eventual convergence to a facet Bell inequality.

Algorithm 1 Constrained Gradient Update for Bell Inequality Coefficients

```

1: Input: coefficients  $\alpha_{\boldsymbol{\mu}}^{\text{in}}$ , gradient step size  $s$ , number of parties  $N$ , input vertices  $V^{\text{in}}$ , maximum iteration steps  $K$ 
2: Output: updated coefficients  $\alpha_{\boldsymbol{\mu}}^{\text{out}}$ , output vertices  $V^{\text{out}}$ 
3: if  $\text{rank}(V^{\text{in}}) = d$  then
4:   Return  $(\alpha_{\boldsymbol{\mu}}^{\text{in}}, V^{\text{in}})$ 
5: end if
6:  $V \leftarrow V^{\text{in}}$ 
7:  $\delta\alpha_{\boldsymbol{\mu}}^{\text{try}} \leftarrow s \frac{\partial \Delta}{\partial \alpha_{\boldsymbol{\mu}}} \Big|_{\alpha_{\boldsymbol{\mu}}=\alpha_{\boldsymbol{\mu}}^{\text{in}}}$ 
8: for  $t = 1$  to  $K$  do
9:    $\alpha_{\boldsymbol{\mu}} \leftarrow \alpha_{\boldsymbol{\mu}}^{\text{in}} + [I - V^T(VV^T)^+V]\delta\alpha_{\boldsymbol{\mu}}^{\text{try}}$ 
10:  Evaluate classical bound at  $\alpha_{\boldsymbol{\mu}}$  to get new vertices  $V^{\text{add}}$ 
11:   $V \leftarrow \text{merge}(V, V^{\text{add}})$ 
12:  if  $V^{\text{in}} \subseteq V$  then
13:    Return  $(\alpha_{\boldsymbol{\mu}}, V)$  as  $(\alpha_{\boldsymbol{\mu}}^{\text{out}}, V^{\text{out}})$ 
14:  end if
15: end for
16: Return  $(\alpha_{\boldsymbol{\mu}}, V)$  as  $(\alpha_{\boldsymbol{\mu}}^{\text{out}}, V^{\text{out}})$ 

```

IV. LOCAL POLYTOPE AND QUANTUM SET FOR (2, 2, 2) SCENARIO

We first consider the (2, 2, 2) scenario as a benchmark to introduce and validate our optimization framework. Our gradient optimization converges to the CHSH inequality in this scenario. The linear functional with only considering the two-body terms is explicitly

$$I = \alpha_{00} \langle A_0 B_0 \rangle + \alpha_{01} \langle A_0 B_1 \rangle + \alpha_{10} \langle A_1 B_0 \rangle + \alpha_{11} \langle A_1 B_1 \rangle, \quad (\text{S21})$$

where $\langle A_k B_l \rangle$ denotes the two-body correlator between measurement A_k on Alice and B_l on Bob satisfying

$$-1 \leq \langle A_k B_l \rangle \leq 1. \quad (\text{S22})$$

The local hidden variable model gives the following constraints on the correlators

$$\begin{aligned} -2 &\leq \langle A_0 B_0 \rangle + \langle A_0 B_1 \rangle + \langle A_1 B_0 \rangle + \langle A_1 B_1 \rangle \leq 2, \\ -2 &\leq \langle A_0 B_0 \rangle - \langle A_0 B_1 \rangle + \langle A_1 B_0 \rangle + \langle A_1 B_1 \rangle \leq 2, \\ -2 &\leq \langle A_0 B_0 \rangle + \langle A_0 B_1 \rangle - \langle A_1 B_0 \rangle + \langle A_1 B_1 \rangle \leq 2, \\ -2 &\leq \langle A_0 B_0 \rangle + \langle A_0 B_1 \rangle + \langle A_1 B_0 \rangle - \langle A_1 B_1 \rangle \leq 2. \end{aligned} \quad (\text{S23})$$

The quantum set of the two-body correlations is represented by [S4, S5]

$$\begin{aligned} -\pi &\leq \arcsin(\langle A_0 B_0 \rangle) + \arcsin(\langle A_0 B_1 \rangle) + \arcsin(\langle A_1 B_0 \rangle) + \arcsin(\langle A_1 B_1 \rangle) \leq \pi, \\ -\pi &\leq \arcsin(\langle A_0 B_0 \rangle) - \arcsin(\langle A_0 B_1 \rangle) + \arcsin(\langle A_1 B_0 \rangle) + \arcsin(\langle A_1 B_1 \rangle) \leq \pi, \\ -\pi &\leq \arcsin(\langle A_0 B_0 \rangle) + \arcsin(\langle A_0 B_1 \rangle) - \arcsin(\langle A_1 B_0 \rangle) + \arcsin(\langle A_1 B_1 \rangle) \leq \pi, \\ -\pi &\leq \arcsin(\langle A_0 B_0 \rangle) + \arcsin(\langle A_0 B_1 \rangle) + \arcsin(\langle A_1 B_0 \rangle) - \arcsin(\langle A_1 B_1 \rangle) \leq \pi. \end{aligned} \quad (\text{S24})$$

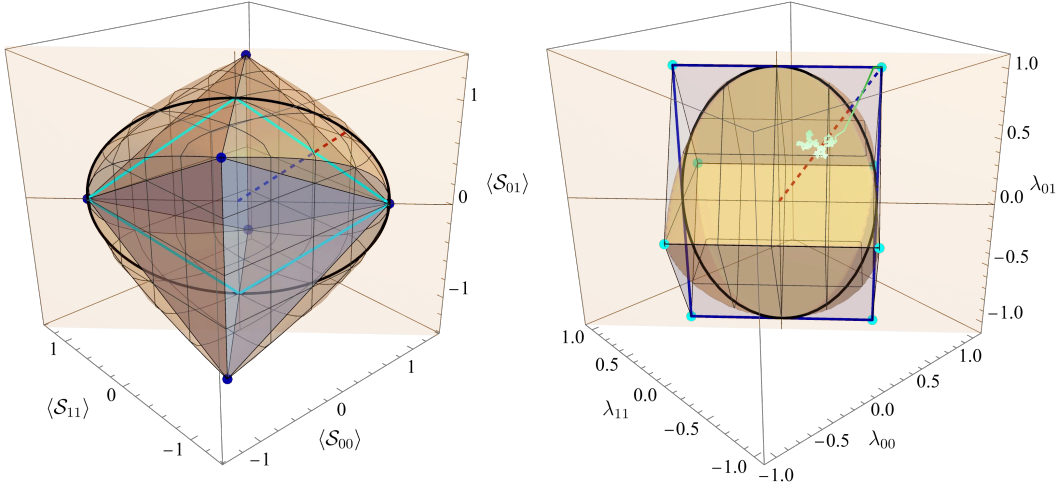


FIG. S2. Local polytope and quantum set for bipartite system. (a) The original local polytope (inside) and quantum set (outside). Four CHSH inequalities correspond to the facets indicated by the blue lines. (b) The dual polytope (outside) and the dual quantum set (inside). The vertices of the polytope are tight Bell inequalities. In both subfigures, the solid curves show a 2D cross section where the largest ratio is obtained. The light-green trajectory shows the convergence of the inequality to one of the CHSH inequalities during the optimization.

Let us consider the symmetric Bell inequality with $\alpha_{01} = \alpha_{10}$. We introduce

$$\langle S_{00} \rangle = \langle A_0 B_0 \rangle, \langle S_{01} \rangle = (\langle A_0 B_1 \rangle + \langle A_1 B_0 \rangle)/2, \langle S_{11} \rangle = \langle A_1 B_1 \rangle, \quad (S25)$$

and obtain the symmetric bipartite Bell inequality

$$I = \alpha_{00} \langle S_{00} \rangle + 2\alpha_{01} \langle S_{01} \rangle + \alpha_{11} \langle S_{11} \rangle \geq \beta_C. \quad (S26)$$

Figure S2(a) shows the local polytope (inner octahedron) and the quantum set (outer convex body) for the symmetric $(2, 2, 2)$ scenario. The local polytope is simplified into

$$|\langle S_{01} \rangle| \leq 1 - |\langle S_{00} \rangle - \langle S_{11} \rangle|/2, \quad (S27)$$

which has six vertices $(S_{00}, S_{01}, S_{11}) = \pm(1, \pm 1, 1)$ and $\pm(1, 0, -1)$ (blue dots). The quantum set by Eq. (S24) is simplified into

$$|\langle S_{01} \rangle(\langle S_{00} \rangle - \langle S_{11} \rangle)| \leq (1 - \langle S_{01} \rangle)^{1/2}[(1 - \langle S_{00} \rangle)^{1/2} + (1 - \langle S_{11} \rangle)^{1/2}]. \quad (S28)$$

Four CHSH inequalities with the largest ratio correspond to the facets of the local polytope. In a 2D cross section, the CHSH inequalities are shown by the cyan lines, and the black curves show the quantum value.

Figure S2(b) shows the polar transformation of both the local polytope (outer hexahedron) and the quantum set (inner convex body) by solving the dual variables λ_{00} , λ_{01} , and λ_{11} from

$$\lambda_{00} \langle S_{00} \rangle + \lambda_{01} \langle S_{01} \rangle + \lambda_{11} \langle S_{11} \rangle \geq -1. \quad (S29)$$

Each tight Bell inequality corresponds to a cyan vertex of the polytope. Four CHSH vertices are $(\lambda_{00}, \lambda_{01}, \lambda_{11}) = \pm(1/2, -1, \pm 1/2)$. The other four vertices are $(\lambda_{00}, \lambda_{01}, \lambda_{11}) = \pm(1, 0, 0)$ and $\pm(0, 0, 1)$. The dual quantum set is given by $\sqrt{(\lambda_{00} - \lambda_{11})^2 + \lambda_{01}^2} \leq 1$ and $(|\lambda_{00} + \lambda_{11}| + |\lambda_{01}|) \leq 1$. We also show the two-dimensional cross section that contains the maximum ratio achieved by the CHSH inequalities represented by the four vertices in the cross section. We show the trajectory during optimization in Fig. S2(b) by the green curve; the step size is chosen as $s = 0.01$. In the initial stage, when the gradient vanishes ($\partial \Delta / \partial \alpha_\mu = 0$), the gradient term in Eq. (S15) is replaced by random noise sampled from a standard normal distribution. We remark the two-dimensional affine projection and the cross section in both subfigures correspond to Fig. S2 (a) and (b) in the main text.

V. TIGHT BELL INEQUITIES FOR $(N, 2, 2)$ AND $(N, 3, 2)$ SCENARIOS WITH SMALL N

In the following, we focus on finding tight PI Bell inequalities involving upto two-body correlators in the $(N, m, 2)$ scenario with $m = 2$ or $m = 3$. For $m = 2$, the linear functional is explicitly

$$I = \alpha_0 \langle \mathcal{S}_0 \rangle + \alpha_1 \langle \mathcal{S}_1 \rangle + \frac{1}{2} \alpha_{00} (\langle \mathcal{S}_0^2 \rangle - N) + \alpha_{01} (\langle \mathcal{S}_0 \mathcal{S}_1 - \mathcal{Z}_{01} \rangle) + \frac{1}{2} \alpha_{11} (\langle \mathcal{S}_1^2 \rangle - N), \quad (\text{S30})$$

where \mathcal{S}_0 , \mathcal{S}_1 and \mathcal{Z}_{01} are classical random variables. To search for tight Bell inequalities, we enumerate the vertices of the local polytope corresponding to local deterministic strategies according to Sec. II. The classical bound β_C is obtained as the minimum value of I over the vertices.

To evaluate the quantum value, we consider the measurements encoded by Eqs. (S7) and (S11). The Bell operator is given by

$$\hat{I}(\boldsymbol{\theta}) = \alpha_0 \hat{\mathcal{S}}_0 + \alpha_1 \hat{\mathcal{S}}_1 + \frac{1}{2} \alpha_{00} (\hat{\mathcal{S}}_0^2 - N) + \frac{1}{2} \alpha_{01} (\hat{\mathcal{S}}_0 \hat{\mathcal{S}}_1 + \hat{\mathcal{S}}_1 \hat{\mathcal{S}}_0 - 2 \hat{\mathcal{Z}}_{01}) + \frac{1}{2} \alpha_{11} (\hat{\mathcal{S}}_1^2 - N). \quad (\text{S31})$$

Plugging the measurement settings (Eqs. (S7) and (S11)) into Eq. (S31), we obtain

$$\begin{aligned} \hat{I}(\boldsymbol{\theta}) = & 2(\alpha_{00} \cos^2 \theta_0 + 2\alpha_{01} \cos \theta_0 \cos \theta_1 + \alpha_{11} \cos^2 \theta_1) \hat{\mathcal{S}}_x + 2(\alpha_{00} \sin^2 \theta_0 + 2\alpha_{01} \sin \theta_0 \sin \theta_1 + \alpha_{11} \sin^2 \theta_1) \hat{\mathcal{S}}_z^2 \\ & + 2[\alpha_{00} \cos \theta_0 \sin \theta_0 + \alpha_{11} \cos \theta_1 \sin \theta_1 + \alpha_{01} (\sin \theta_0 \cos \theta_1 + \cos \theta_0 \sin \theta_1)] (\hat{\mathcal{S}}_x \hat{\mathcal{S}}_z + \hat{\mathcal{S}}_z \hat{\mathcal{S}}_x) \\ & + 2(\alpha_0 \cos \theta_0 + \alpha_1 \cos \theta_1) \hat{\mathcal{S}}_x + 2(\alpha_0 \sin \theta_0 + \alpha_1 \sin \theta_1) \hat{\mathcal{S}}_z - \frac{1}{2} \alpha_{00} N - \alpha_{01} N \cos(\theta_0 - \theta_1) - \frac{1}{2} \alpha_{11} N. \end{aligned} \quad (\text{S32})$$

The minimal quantum value is obtained by searching over θ_0 and θ_1 to minimize the ground state energy of $\hat{I}(\boldsymbol{\theta})$.

TABLE I: The ratio and the corresponding coefficients for nontrivial facet Bell inequality for $N = 4$, $m = 2$.

| $\Delta_{4,2}$ | β_Q | β_C | $(\alpha_0, \alpha_1, \alpha_{00}, \alpha_{01}, \alpha_{11})$ |
|----------------|-----------|-----------|---|
| 1.11303 | -20.03447 | -18 | (0, 0, 6, 2, -1) |
| 1.02579 | -30.77363 | -30 | (12, 3, 6, 2, -1) |
| 1.01391 | -54.75094 | -54 | (12, 6, 12, 8, -1) |
| 1.01339 | -42.56235 | -42 | (12, 9, 6, 6, 1) |

TABLE II: The ratio and the corresponding coefficients for nontrivial facet Bell inequality for $N = 5$, $m = 2$.

| $\Delta_{5,2}$ | β_Q | β_C | $(\alpha_0, \alpha_1, \alpha_{00}, \alpha_{01}, \alpha_{11})$ |
|----------------|------------|-----------|---|
| 1.05904 | -84.72301 | -80 | (20, 4, 20, 5, -2) |
| 1.01769 | -24.42458 | -24 | (6, 6, 1, 2, 1) |
| 1.01515 | -10.15146 | -10 | (2, 0, 1, 1, 1) |
| 1.01117 | -70.78216 | -70 | (20, 14, 5, 5, 1) |
| 1.00805 | -201.61020 | -200 | (60, 24, 30, 15, -2) |
| 1.00747 | -130.97171 | -130 | (36, 28, 8, 10, 3) |
| 1.00679 | -161.08648 | -160 | (60, 12, 20, 5, -2) |
| 1.00138 | -400.55077 | -400 | (60, 36, 60, 45, 2) |

TABLE III: The ratio and the corresponding coefficients for nontrivial facet inequalities for $N = 6$, $m = 2$

| $\Delta_{6,2}$ | β_Q | β_C | $(\alpha_0, \alpha_1, \alpha_{00}, \alpha_{01}, \alpha_{11})$ |
|----------------|-----------|-----------|---|
| 1.05884 | -63.53040 | -60 | (0, 0, 15, 3, -1) |
| 1.02444 | -92.19967 | -90 | (30, 5, 15, 3, -1) |
| 1.02153 | -12.25837 | -12 | (2, 0, 1, 1, 1) |
| 1.01628 | -16.26044 | -16 | (4, 2, 1, 1, 1) |

(continued on next page)

| (continued from previous page) | | | |
|--------------------------------|------------|-----------|---|
| $\Delta_{6,2}$ | β_Q | β_C | $(\alpha_0, \alpha_1, \alpha_{00}, \alpha_{01}, \alpha_{11})$ |
| 1.01616 | -42.67892 | -42 | (9, 9, 1, 2, 1) |
| 1.00870 | -121.04430 | -120 | (30, 20, 5, 5, 1) |
| 1.00804 | -226.80917 | -225 | (54, 41, 8, 10, 3) |
| 1.00740 | -157.15448 | -156 | (37, 17, 23, 12, 1) |
| 1.00616 | -112.69001 | -112 | (26, 12, 17, 9, 1) |
| 1.00544 | -48.26112 | -48 | (13, 5, 4, 3, 2) |
| 1.00517 | -165.85362 | -165 | (40, 20, 20, 12, 1) |
| 1.00471 | -24.11309 | -24 | (5, 1, 3, 2, 1) |
| 1.00408 | -39.15927 | -39 | (12, 3, 4, 2, 1) |
| 1.00381 | -195.74390 | -195 | (60, 20, 20, 8, -1) |
| 1.00290 | -240.69671 | -240 | (45, 15, 45, 18, -1) |
| 1.00224 | -70.15691 | -70 | (18, 12, 3, 3, 1) |
| 1.00216 | -180.38922 | -180 | (60, 10, 15, 3, -1) |
| 1.00138 | -300.41277 | -300 | (0, 0, 45, 27, 1) |
| 1.00065 | -129.08436 | -129 | (24, 20, 12, 12, 5) |
| 1.00041 | -273.11285 | -273 | (60, 32, 36, 24, 5) |

For $m = 2$, the `cddlib` [S6] is used to enumerate facets of the local polytope, and the ratio $\Delta_{N,2}$ is evaluated for each facet Bell inequality. Our gradient optimization converges to one facet Bell inequality. For $N = 3$, there is a single nontrivial facet Bell inequalities $(6, 2, 6, 3, -2)$ with the maximum ratio $\Delta_{3,2}^{\max} = 1.11303$. We present in Tables I, II, and III the ratios for all nontrivial facet Bell inequalities in the $(N, 2, 2)$ scenario for $N = 4, 5$, and 6, respectively. We find 4, 8, and 20 inequalities with the ratio $\Delta_{N,2} > 1$. For $N = 5$ and 6, the ratio of the facet Bell inequality $(2, 0, 1, 1, 1)$ is larger than 1. As the number of parties N increases, this Bell inequality continues to achieve the maximum ratio when compared against all facet Bell inequalities within the fixed $(N, 2, 2)$ scenario.

For the $(N, 3, 2)$ scenario, the linear functional is

$$I = \alpha_0 \langle \mathcal{S}_0 \rangle + \alpha_1 \langle \mathcal{S}_1 \rangle + \alpha_2 \langle \mathcal{S}_2 \rangle + \frac{1}{2} \alpha_{00} (\langle \mathcal{S}_0^2 \rangle - N) + \frac{1}{2} \alpha_{11} (\langle \mathcal{S}_1^2 \rangle - N) + \frac{1}{2} \alpha_{22} (\langle \mathcal{S}_2^2 \rangle - N) + \alpha_{01} (\langle \mathcal{S}_0 \mathcal{S}_1 - \mathcal{Z}_{01} \rangle) + \alpha_{02} (\langle \mathcal{S}_0 \mathcal{S}_2 - \mathcal{Z}_{02} \rangle) + \alpha_{12} (\langle \mathcal{S}_1 \mathcal{S}_2 - \mathcal{Z}_{12} \rangle), \quad (\text{S33})$$

and the Bell operator $\hat{I}(\theta)$ is constructed similarly to Eq. (S31) by introducing $\hat{\mathcal{S}}_0 = 2 \cos \theta_0 \hat{S}_z + 2 \sin \theta_0 \hat{S}_x$, $\hat{\mathcal{S}}_1 = 2 \cos \theta_1 \hat{S}_z + 2 \sin \theta_1 \hat{S}_x$, $\hat{\mathcal{S}}_2 = 2 \cos \theta_2 \hat{S}_z + 2 \sin \theta_2 \hat{S}_x$, $\hat{\mathcal{Z}}_{01} = N \cos(\theta_0 - \theta_1)$, $\hat{\mathcal{Z}}_{02} = N \cos(\theta_0 - \theta_2)$, and $\hat{\mathcal{Z}}_{12} = N \cos(\theta_1 - \theta_2)$.

We list the ratios over all the facet Bell inequalities with $N \leq 4$ using `cddlib` [S6]. The results of the ratio and the nontrivial facet Bell inequalities are given in Tables. IV, V, and VI for $N = 2, 3$, and 4, respectively. For $N = 2$ and 3, the maximum ratio for $m = 3$ is the same as that for $m = 2$, but a larger ratio is obtained when $N \geq 4$. For $N = 4$, the ten largest ratios and their corresponding coefficients are shown. The Bell inequality with $\alpha_{\mu} = (0, 0, 0, 3, 3, 2, 3, 0, -1)$ has a larger ratio $\Delta_{4,3}^{\max} = 1.11760$ compared to $\Delta_{4,2}^{\max} = 1.11303$ by $\alpha_{\mu} = (0, 0, 6, 2, -1)$. Since `cddlib` [S6] becomes infeasible for larger values of N , we instead employ our gradient-based method to search for Bell inequalities and obtain the inequalities listed in Table II of the main text.

TABLE IV: The ratio and the corresponding coefficients for nontrivial facet Bell inequalities for $N = 2, m = 3$.

| $\Delta_{2,3}$ | β_Q | β_C | $(\alpha_0, \alpha_1, \alpha_2, \alpha_{00}, \alpha_{01}, \alpha_{02}, \alpha_{11}, \alpha_{12}, \alpha_{22})$ |
|----------------|--------------|-----------|--|
| $\sqrt{2}$ | $-2\sqrt{2}$ | -2 | (0, 0, 0, 1, 1, 0, -1, 0, 0) |
| $\sqrt{2}$ | $-4\sqrt{2}$ | -4 | (0, 0, 0, 0, 1, 1, 0, 1, -2) |
| $5/4$ | -10 | -8 | (2, 1, 1, 2, 2, 2, -2, 1, -2) |

TABLE V: The ratio and the corresponding coefficients for nontrivial facet Bell inequalities for $N = 3, m = 3$.

| $\Delta_{3,3}$ | β_Q | β_C | $(\alpha_0, \alpha_1, \alpha_2, \alpha_{00}, \alpha_{01}, \alpha_{02}, \alpha_{11}, \alpha_{12}, \alpha_{22})$ |
|----------------|-----------|-----------|--|
| 1.11303 | -20.03447 | -18 | (4, 2, 2, 2, 2, 0, 1, -2) |

(continued on next page)

| <i>(continued from previous page)</i> | | | |
|---------------------------------------|-----------|-----------|--|
| $\Delta_{3,3}$ | β_Q | β_C | $(\alpha_0, \alpha_1, \alpha_2, \alpha_{00}, \alpha_{01}, \alpha_{02}, \alpha_{11}, \alpha_{12}, \alpha_{22})$ |
| 1.11303 | -20.03447 | -18 | (6, 2, 0, 6, 3, 0, -2, 0, 0) |
| 1.10033 | -46.21398 | -42 | (6, 6, 4, 6, 6, 3, 0, 3, -4) |
| 1.09643 | -52.62880 | -48 | (12, 6, 2, 12, 6, 0, 0, 3, -2) |
| 1.09545 | -32.86344 | -30 | (6, 6, 2, 3, 3, 3, 0, -2) |
| 1.09395 | -32.81848 | -30 | (6, 4, 2, 4, 4, 3, 2, 0, -2) |
| 1.07606 | -22.59729 | -21 | (6, 2, 0, 6, 2, 1, 0, -1, -1) |
| 1.07157 | -16.07351 | -15 | (2, 2, 0, 2, 2, 1, 2, -1, -1) |
| 1.06941 | -38.49887 | -36 | (6, 4, 2, 6, 6, 3, -2, 2, -2) |
| 1.05448 | -15.81716 | -15 | (4, 2, 0, 3, 1, 1, 1, -1, -1) |
| 1.05099 | -63.05926 | -60 | (6, 6, 4, 12, 9, 6, -2, 4, -4) |
| 1.04734 | -21.99416 | -21 | (6, 2, 0, 6, 1, 2, 0, -1, -1) |
| 1.03970 | -11.43666 | -11 | (2, 2, 0, 2, 0, 1, 2, -1, -1) |
| 1.03825 | -37.37713 | -36 | (4, 2, 2, 8, 5, 5, -2, 2, -2) |
| 1.03806 | -37.37011 | -36 | (12, 4, 4, 6, 3, 3, -2, 1, -2) |
| 1.02985 | -30.89545 | -30 | (6, 2, 0, 3, 3, 3, -2, 3, 3) |
| 1.02831 | -30.84942 | -30 | (6, 2, 0, 4, 3, 4, -2, 2, 2) |
| 1.02498 | -30.74945 | -30 | (4, 2, 2, 0, 4, 2, 6, 3, -2) |
| 1.01935 | -36.69651 | -36 | (10, 4, 0, 9, 1, 4, 1, -2, -2) |
| 1.00897 | -36.32307 | -36 | (6, 2, 0, 2, 3, 4, -2, 4, 6) |

TABLE VI: The ten largest ratio and the corresponding coefficients for nontrivial facet Bell inequalities for $N = 4$, $m = 3$.

| $\Delta_{4,3}$ | β_Q | β_C | $(\alpha_0, \alpha_1, \alpha_2, \alpha_{00}, \alpha_{01}, \alpha_{02}, \alpha_{11}, \alpha_{12}, \alpha_{22})$ |
|----------------|------------|-----------|--|
| 1.11760 | -33.52793 | -30 | (0, 0, 0, 3, 3, 2, 3, 0, -1) |
| 1.11303 | -20.03447 | -18 | (0, 0, 0, 6, 2, 0, -1, 0, 0) |
| 1.11303 | -40.06894 | -36 | (0, 0, 0, 6, 3, 3, 0, 1, -2) |
| 1.11303 | -20.03447 | -18 | (0, 0, 0, 1, 2, 1, 1, 1, -1) |
| 1.09879 | -72.52003 | -66 | (0, 0, 0, 18, 6, 0, 0, 2, -1) |
| 1.09672 | -92.12404 | -84 | (0, 0, 0, 12, 9, 5, 0, 3, -4) |
| 1.09661 | -65.79685 | -60 | (c) |
| 1.09594 | -414.26432 | -378 | (9, 6, 3, 42, 39, 24, 6, 17, -19) |
| 1.09457 | -637.03913 | -582 | (12, 12, 6, 60, 60, 36, 12, 28, -29) |
| 1.09373 | -413.43150 | -378 | (12, 6, 0, 12, 20, 36, -19, 24, 36) |

VI. RESULTS FOR $(N, m, 2)$ SCENARIO IN THE THERMODYNAMIC LIMIT $N \rightarrow \infty$

The permutation symmetry allows a rigorous mean-field solution in the thermodynamic limit. In the classical case, the bound can be obtained from a continuous-variable approximation at large N . In the quantum case, the value reduces to computing the ground-state energy of a Lipkin-Meshkov-Glick-type Hamiltonian [S1], which can be treated using the semiclassical method. In the large- N limit, the collective-spin model admits a semiclassical description in terms of spin-coherent states: the leading contribution is captured by a mean-field energy functional, with quantum fluctuations entering as $1/N$ corrections.

For both classical and quantum cases, we introduce continuous variables $s_k = \langle \mathcal{S}_k \rangle / N$ and $z_{kl} = \langle \mathcal{Z}_{kl} \rangle / N$. In the thermodynamic limit, the state concentrates on a single-point support characterized by certain s_k and z_{kl} with the two-body correlator approaching $\langle \mathcal{S}_k \mathcal{S}_l \rangle = N^2 s_k s_l$. The linear functional Eq. (S2) becomes

$$I = \frac{N^2}{2} \sum_{k,l=0}^{m-1} \alpha_{kl} s_k s_l + N \left(\sum_{k=0}^{m-1} \alpha_k s_k - \frac{1}{2} \sum_{k,l=0}^{m-1} \alpha_{kl} z_{kl} \right), \quad (\text{S34})$$

where the quadratic terms have N^2 scaling and the linear terms have N scaling.

For the classical case, the local polytope is $-1 + |s_k + s_l| \leq z_{kl} \leq 1 - |s_k - s_l|$ when $k \neq l$ and $z_{kk} = 1$. For quantum case, we introduce the semiclassical variables $s_x = 2S_x/N$ and $s_z = 2S_z/N$ and express $s_k = \cos \theta_k s_z + \sin \theta_k s_x$ and $z_{kl} = \cos(\theta_k - \theta_l)$. We eliminate θ_k and obtain the convex set as $z_{kl}^2 + s_k^2 + s_l^2 - 2z_{kl}s_k s_l \leq 1$. Therefore, the

classical bound and the minimal quantum value in the thermodynamic limit $N \rightarrow \infty$ are converted to the following optimization

$$\beta_{C/Q} = \min_{(\mathbf{s}, \mathbf{z}) \in \mathcal{N}_{C/Q}} \frac{N^2}{2} \sum_{k,l=0}^{m-1} \alpha_{kl} s_k s_l + N \left(\sum_{k=0}^{m-1} \alpha_k s_k - \frac{1}{2} \sum_{k,l=0}^{m-1} \alpha_{kl} z_{kl} \right), \quad (\text{S35})$$

where $\mathbf{s} = (s_0, \dots, s_{m-1})$ collects the continuous single-site variables and $\mathbf{z} = (z_{kl})_{k,l=0}^{m-1}$ collects the continuous two-body variables. The corresponding classical and quantum feasible regions are given by

$$\mathcal{N}_C = \{(\mathbf{s}, \mathbf{z}) \mid -1 \leq s_k \leq 1, z_{kk} = 1, -1 \leq z_{kl} \leq 1, -1 + |s_k + s_l| \leq z_{kl} \leq 1 - |s_k - s_l|\}, \quad (\text{S36})$$

and

$$\mathcal{N}_Q = \{(\mathbf{s}, \mathbf{z}) \mid z_{kk} = 1, \begin{pmatrix} 1 & s_k & s_l \\ s_k & 1 & z_{kl} \\ s_l & z_{kl} & 1 \end{pmatrix} \succcurlyeq 0\}, \quad (\text{S37})$$

respectively. Note that $\beta_{C/Q}$ is linear on \mathbf{z} , and thus \mathbf{z} should take the extreme value on both the classical local polytope and quantum convex set.

We can first optimize the classical bound and the quantum value over \mathbf{z} . For the classical bound, z_{kl} takes the extreme values $-1 + |s_k + s_l|$ or $1 - |s_k - s_l|$ according to $\alpha_{kl} < 0$ or $\alpha_{kl} > 0$, respectively. The classical bound is

$$\beta_C = \min_{s_k \in [-1, 1]} \frac{N^2}{2} \sum_{k,l=0}^{m-1} \alpha_{kl} s_k s_l + N \left[\sum_{k=0}^{m-1} \alpha_k s_k - \frac{1}{2} \sum_{k=0}^{m-1} \alpha_{kk} - \frac{1}{2} \sum_{k \neq l, l=0}^{m-1} |\alpha_{kl}| (1 - |s_k - \text{sign}(\alpha_{kl}) s_l|) \right]. \quad (\text{S38})$$

For the quantum value, z_{kl} takes the extreme values $s_k s_l - \sqrt{(1 - s_k^2)(1 - s_l^2)}$ or $s_k s_l + \sqrt{(1 - s_k^2)(1 - s_l^2)}$ according to $\alpha_{kl} < 0$ or $\alpha_{kl} > 0$, respectively. The quantum value is

$$\beta_Q = \min_{s_k \in [-1, 1]} \frac{N^2}{2} \sum_{k,l=0}^{m-1} \alpha_{kl} s_k s_l + N \left[\sum_{k=0}^{m-1} \alpha_k s_k - \frac{1}{2} \sum_{k=0}^{m-1} \alpha_{kk} - \frac{1}{2} \sum_{k \neq l, l=0}^{m-1} (\alpha_{kl} s_k s_l + |\alpha_{kl}| \sqrt{(1 - s_k^2)(1 - s_l^2)}) \right]. \quad (\text{S39})$$

In the thermodynamic limit $N \rightarrow \infty$, the quadratic form in the first line scales with N^2 while the linear form in the second line scales with N . Note the quadratic form take the same values in both quantum and classical cases. To obtain nontrivial ratio ($\Delta > 1$), we require (1) α_{kl} is positive semidefinite, and (2) $\sum_{k,l=0}^{m-1} \alpha_{kl} s_k s_l = 0$, which gives an extra constraint on s_k . Then we rewrite the quadratic terms into sum of squares

$$\sum_{k,l=0}^{m-1} \alpha_{kl} s_k s_l = \sum_{k=0}^{r-1} \left(\sum_{k=0}^{m-1} \gamma_{kl} s_l \right)^2 \quad (\text{S40})$$

with r as the rank of α_{kl} , which introduces r constraint $\sum_{k=0}^{m-1} \gamma_{kl} s_l = 0$ for the following linear programming or SDP

$$\beta_{C/Q} = \min_{\substack{(\mathbf{s}, \mathbf{z}) \in \mathcal{N}_{C/Q}, \\ \boldsymbol{\gamma}^\top \mathbf{s} = 0}} N \left(\sum_{k=0}^{m-1} \alpha_k s_k - \frac{1}{2} \sum_{k,l=0}^{m-1} \sum_{j=1}^r \gamma_{kj} \gamma_{lj} z_{kl} \right), \quad (\text{S41})$$

where $\boldsymbol{\gamma}$ collects the variables γ_{kl} . This linear cost function implies that both the classical bound and the quantum value are attained at extreme points.

Since $\alpha_{kl} \succeq 0$, there exists a matrix $\{\gamma_{ij}\} \in \mathbb{R}^{r \times m}$ such that

$$\alpha_{kl} = \sum_{j=0}^{r-1} \gamma_{jl} \gamma_{jk} \quad (\text{S42})$$

We can express the quadratic form as a sum of squares:

$$\sum_{k,l} \alpha_{kl} s_k s_l = \sum_{j=0}^{r-1} \left(\sum_{l=0}^{m-1} \gamma_{jl} s_l \right)^2. \quad (\text{S43})$$

The condition $\sum_{k,l=0}^{m-1} \alpha_{kl} s_k s_l = 0$ is thus equivalent to the r independent linear constraints

$$\sum_{l=0}^{m-1} \gamma_{jl} s_l = 0, \quad j = 0, \dots, r-1. \quad (\text{S44})$$

These linear relations define an affine subspace in the space of correlators, and we optimize the linear functional over the intersection of this subspace with the classical local polytope and with the quantum convex set. The classical bound then reduces to a linear program, while the quantum value can be computed by a semidefinite program, both under the linear constraints (S44).

The rank $r = \text{rank}(\alpha_{kl})$ equals the number of independent linear constraints imposed simultaneously on the classical and quantum correlation sets. As r increases, both feasible sets intersect with more independent hyperplanes and therefore shrink. Adding unnecessary extra constraints can only reduce, or at best leave unchanged, the ratio between the maximal quantum and classical values, since such constraints typically lower both optima in a similar way without increasing their separation.

In particular, to remove the common contribution N^2 it suffices to impose at least one nontrivial quadratic constraint. Among all non-zero positive semidefinite α_{kl} , the smallest possible rank is $r = 1$. In that case α_{kl} has the form

$$\alpha_{kl} = \gamma_k \gamma_l, \quad (\text{S45})$$

for some real vector $\gamma = (\gamma_0, \gamma_1, \dots, \gamma_{m-1})^\top \in \mathbb{R}^m$, i.e. α_{kl} is a rank-one projector. This choice imposes exactly one independent linear constraint on \mathbf{s} , while higher-rank matrices would impose additional constraints that restrict the classical and quantum feasible sets simultaneously without improving their relative separation. We therefore restrict our attention, without loss of generality for the maximization of $\Delta_{\infty, m}$, to rank-one positive semidefinite matrices α . Under the rank-one constraint, Eq. (S41) reduces to

$$\beta_{C/Q} = \min_{\substack{(\mathbf{s}, \mathbf{z}) \in \mathcal{N}_{C/Q}, \\ \gamma^\top \mathbf{s} = 0}} N \left(\sum_{k=0}^{m-1} \alpha_k s_k - \frac{1}{2} \sum_{k,l=0}^{m-1} \gamma_k \gamma_l z_{kl} \right). \quad (\text{S46})$$

Using the symmetry group of the polytope, we assume all γ_k positive, which leads to $z_{kl} = 1 - |s_k - s_l|$ in the classical case and $z_{kl} = s_k s_l + \sqrt{(1 - s_k^2)(1 - s_l^2)}$ in the quantum case. We simplify the classical bound by Eq. (S38) into

$$\beta_C = \min_{s_k \in [-1, 1]} \frac{N^2}{2} \sum_{k,l=0}^{m-1} \alpha_{kl} s_k s_l + N \left[\sum_{k=0}^{m-1} \alpha_k s_k - \frac{1}{2} \sum_{k=0}^{m-1} \alpha_{kk} - \frac{1}{2} \sum_{k \neq l, l=0}^{m-1} \alpha_{kl} (1 - |s_k - s_l|) \right] \quad (\text{S47})$$

$$= \min_{s_k \in [-1, 1]} \frac{N^2}{2} \sum_{k,l=0}^{m-1} \alpha_{kl} s_k s_l + N \left[\sum_{k=0}^{m-1} \alpha_k s_k - \frac{1}{2} \sum_{k,l=0}^{m-1} \alpha_{kl} (1 - |s_k - s_l|) \right] \quad (\text{S48})$$

$$= \min_{\substack{s_k \in [-1, 1], \\ \gamma^\top \mathbf{s} = 0}} N \left[\sum_{k=0}^{m-1} \alpha_k s_k - \frac{1}{2} \sum_{k,l=0}^{m-1} \gamma_k \gamma_l (1 - |s_k - s_l|) \right], \quad (\text{S49})$$

where in the second line we merge the summations of the diagonal and the off-diagonal elements, and in the last line, we impose the constraint that the N^2 term vanishes. Also, the quantum value by Eq. (S39) is simplified into

$$\beta_Q = \min_{s_k \in [-1, 1]} \frac{N^2}{2} \sum_{k,l=0}^{m-1} \alpha_{kl} s_k s_l + N \left[\sum_{k=0}^{m-1} \alpha_k s_k - \frac{1}{2} \sum_{k=0}^{m-1} \alpha_{kk} - \frac{1}{2} \sum_{k \neq l, l=0}^{m-1} (\alpha_{kl} s_k s_l + \alpha_{kl} \sqrt{(1 - s_k^2)(1 - s_l^2)}) \right] \quad (\text{S50})$$

$$= \min_{s_k \in [-1, 1]} \frac{N^2}{2} \sum_{k,l=0}^{m-1} \alpha_{kl} s_k s_l + N \left[\sum_{k=0}^{m-1} \alpha_k s_k - \frac{1}{2} \sum_{k,l=0}^{m-1} (\alpha_{kl} s_k s_l + \alpha_{kl} \sqrt{(1 - s_k^2)(1 - s_l^2)}) \right] \quad (\text{S51})$$

$$= \min_{\substack{s_k \in [-1, 1], \\ \gamma^\top \mathbf{s} = 0}} N \left[\sum_{k=0}^{m-1} \alpha_k s_k - \frac{1}{2} \left(\sum_{k=0}^{m-1} \gamma_k s_k \right)^2 - \frac{1}{2} \left(\sum_{k=0}^{m-1} \gamma_k \sqrt{1 - s_k^2} \right)^2 \right] \quad (\text{S52})$$

$$= \min_{\substack{s_k \in [-1, 1], \\ \gamma^\top \mathbf{s} = 0}} N \left[\sum_{k=0}^{m-1} \alpha_k s_k - \frac{1}{2} \left(\sum_{k=0}^{m-1} \gamma_k \sqrt{1 - s_k^2} \right)^2 \right], \quad (\text{S53})$$

where in the last we use the fact that $\gamma^\top \mathbf{s} = \sum_{k=0}^{m-1} \gamma_k s_k = 0$.

To satisfy the constraint $\gamma^\top \mathbf{s} = 0$, we employ a reversing symmetry in γ and α . For even m , we parameterize the first $m/2$ elements with index j starting from 1 to $m/2$. The whole vectors are

$$\gamma = (\gamma_1, \gamma_2, \dots, \gamma_{m/2}, \gamma_1, \gamma_2, \dots, \gamma_{m/2}), \quad (\text{S54})$$

$$\alpha = (-\alpha_1, -\alpha_2, \dots, -\alpha_{m/2}, \alpha_1, \alpha_2, \dots, \alpha_{m/2}). \quad (\text{S55})$$

For the minimization in the classical bound and the quantum value, we require that

$$\mathbf{s} = (s_1, s_2, \dots, s_{m/2}, -s_1, -s_2, \dots, -s_{m/2}). \quad (\text{S56})$$

For odd m , it is similar by including an additional element

$$\gamma = (\gamma_0, \gamma_1, \gamma_2, \dots, \gamma_{(m-1)/2}, \gamma_1, \gamma_2, \dots, \gamma_{(m-1)/2}), \quad (\text{S57})$$

$$\alpha = (0, -\alpha_1, -\alpha_2, \dots, -\alpha_{m/2}, \alpha_1, \alpha_2, \dots, \alpha_{m/2}), \quad (\text{S58})$$

$$\mathbf{s} = (0, s_1, s_2, \dots, s_{m/2}, -s_1, -s_2, \dots, -s_{m/2}). \quad (\text{S59})$$

Then the constraint $\gamma^\top \mathbf{s} = 0$ is satisfied. We assume α_j for $1 \leq j \leq \lfloor m/2 \rfloor$ are positive and ordered increasingly, and consequently we obtain $s_j \in [0, 1]$ for $1 \leq j \leq \lfloor m/2 \rfloor$ for the minimization. For convenience, we represent the classical bound (S49) and the quantum value (S53) into

$$\beta_C = \frac{Nm^2}{2} \min_{s_j \in [0, 1]} g(\mathbf{s}), \quad (\text{S60})$$

$$\beta_Q = \frac{Nm^2}{2} \min_{s_j \in [0, 1]} f(\mathbf{s}), \quad (\text{S61})$$

where the two functions are explicitly

$$g(\mathbf{s}) = \begin{cases} -\frac{4}{m^2} [\sum_{s_j=1} \alpha_j + (\sum_{s_i=0} \gamma_i)^2], & \text{even } m \\ -\frac{4}{m^2} [\sum_{s_j=1} \alpha_j + (\frac{\gamma_0}{2} + \sum_{s_i=0} \gamma_i)^2], & \text{odd } m, \end{cases} \quad (\text{S62})$$

and

$$f(\mathbf{s}) = \begin{cases} -\frac{4}{m^2} [\sum_{j=1}^{m/2} \alpha_j s_j + (\sum_{j=1}^{m/2} \gamma_j \sqrt{1-s_j^2})^2], & \text{even } m \\ -\frac{4}{m^2} [\sum_{j=1}^{(m-1)/2} \alpha_j s_j + (\frac{\gamma_0}{2} + \sum_{j=1}^{(m-1)/2} \gamma_j \sqrt{1-s_j^2})^2], & \text{odd } m. \end{cases} \quad (\text{S63})$$

For the classical bound β_C , s_j takes either 0 or 1. We denote these minimum as $g^* = g(\mathbf{s}^*)$ and $f^* = f(\mathbf{s}^*)$. Note that $\mathbf{s}^* = \{s_j^*\}_j$ are different for the quantum and classical cases. For the classical case, the elements of s_j^* are either 0 or 1.

To find the optimal choice of \mathbf{s}^* for the minimum quantum value, we introduce

$$c = \begin{cases} \frac{2}{m} \sum_{j=1}^{m/2} \gamma_j \sqrt{1-s_j^2}, & \text{even } m \\ \frac{2}{m} \left(\frac{\gamma_0}{2} + \sum_{j=1}^{(m-1)/2} \gamma_j \sqrt{1-s_j^2} \right), & \text{odd } m. \end{cases} \quad (\text{S64})$$

To minimize $f(\mathbf{s})$, each s_j should be chosen according to

$$\frac{\partial f}{\partial s_j} = -\frac{4}{m^2} [\alpha_j - \gamma_j \frac{mc s_j}{\sqrt{(1-s_j^2)}}, \quad (\text{S65})$$

which gives

$$s_j^* = \frac{1}{\sqrt{1 + m^2 c^2 \gamma_j^2 / \alpha_j^2}}. \quad (\text{S66})$$

Plugging Eq. (S66) into Eq. (S64), we obtain a self-consistent equation to determine c as

$$1 = \begin{cases} 2 \sum_{j=1}^{m/2} \frac{\gamma_j^2}{\sqrt{\alpha_j^2 + m^2 c^2 \gamma_j^2}}, & \text{even } m \\ \gamma_0^2 + 2 \sum_{j=1}^{(m-1)/2} \frac{\gamma_j^2}{\sqrt{\alpha_j^2 + m^2 c^2 \gamma_j^2}}, & \text{odd } m. \end{cases} \quad (\text{S67})$$

We denote the solution to the above self-consistent equation as $c = c^*$.

Since the algebra equation (S67) does not allow an explicit solution for c^* , we first relax c as a free parameter not determined by the above self-consistent equation. We plug the solution Eq. (S66) into Eq. (S63) and obtain

$$f(\mathbf{s}^*, c) = \begin{cases} -\frac{4}{m^2} \sum_{j=1}^{m/2} \frac{\alpha_j^2}{\sqrt{\alpha_j^2 + m^2 c^2 \gamma_j^2}} - \frac{4}{m^2} \left(\sum_{j=1}^{m/2} \gamma_j \frac{mc\gamma_j}{\sqrt{\alpha_j^2 + m^2 c^2 \gamma_j^2}} \right)^2, & \text{even } m \\ -\frac{4}{m^2} \sum_{j=1}^{(m-1)/2} \frac{\alpha_j^2}{\sqrt{\alpha_j^2 + m^2 c^2 \gamma_j^2}} - \frac{4}{m^2} \left(\frac{\gamma_0}{2} + \sum_{j=1}^{(m-1)/2} \gamma_j \frac{mc\gamma_j}{\sqrt{\alpha_j^2 + m^2 c^2 \gamma_j^2}} \right)^2, & \text{odd } m. \end{cases} \quad (\text{S68})$$

We continue to optimize the ratio for even and odd m in the following two subsections, respectively.

A. General even m

We are now ready to consider general even m . To ensure that more vertices saturate the classical bound, we require that

$$g^* = -\frac{4}{m^2} \left[\left(\sum_{i=1}^p \gamma_i \right)^2 + \sum_{j=p+1}^{m/2} \alpha_j \right], \text{ for any } 0 \leq p \leq m/2, \quad (\text{S69})$$

from which we solve all α_k as

$$\alpha_k = \left(\sum_{i=1}^k \gamma_i \right)^2 - \left(\sum_{i=1}^{k-1} \gamma_i \right)^2 = 2\gamma_k \left(\sum_{i=1}^k \gamma_i \right) - \gamma_k^2. \quad (\text{S70})$$

The following $m/2 + 1$ vertices lie on this inequality

$$\mathbf{s}_p = \left(\underbrace{0, \dots, 0}_{p \text{ zeros}}, \underbrace{1, \dots, 1}_{\frac{m}{2}-p \text{ ones}}, \underbrace{0, \dots, 0}_{p \text{ zeros}}, \underbrace{-1, \dots, -1}_{\frac{m}{2}-p \text{ minus ones}} \right), 0 \leq p \leq m/2. \quad (\text{S71})$$

For each \mathbf{s}_k , we can fully determine $z_{kl} = 1 - |\mathbf{s}_k - \mathbf{s}_l|$.

The classical bound is $g^* = -4 \left(\sum_{i=1}^{m/2} \gamma_i \right)^2 / m^2$. With α_k , we rewrite the quantum value as

$$f(\mathbf{s}) = -\frac{4}{m^2} \left\{ \sum_{j=1}^{m/2} [2\gamma_j \left(\sum_{i=1}^j \gamma_i \right) - \gamma_j^2] s_j + \left[\sum_{j=1}^{m/2} \gamma_j \sqrt{1 - s_j^2} \right]^2 \right\}. \quad (\text{S72})$$

The optimal s_j^* becomes

$$s_j^* = \frac{1}{\sqrt{1 + m^2 c^{*2} / (\gamma_j + 2 \sum_{i=1}^{j-1} \gamma_i)^2}}, \quad (\text{S73})$$

and the self-consistent equation (S67) becomes

$$1 = 2 \sum_{j=1}^{m/2} \frac{\gamma_j}{\sqrt{(\gamma_j + 2 \sum_{i=1}^{j-1} \gamma_i)^2 + m^2 c^{*2}}}. \quad (\text{S74})$$

We continue to enhance the ratio Δ by optimizing the coefficients γ_j . We relax c as a free parameter and represent the ratio as

$$\Delta(\boldsymbol{\gamma}, c) = \sum_{j=1}^{m/2} \frac{1}{\left(\sum_{i=1}^{m/2} \gamma_i\right)^2} \frac{\gamma_j(\gamma_j + 2 \sum_{i=1}^{j-1} \gamma_i)^2}{\sqrt{(\gamma_j + 2 \sum_{i=1}^{j-1} \gamma_i)^2 + m^2 c^2}} + \left(\sum_{j=1}^{m/2} \frac{\gamma_j}{\sum_{i=1}^{m/2} \gamma_i} \frac{mc}{\sqrt{(\gamma_j + 2 \sum_{i=1}^{j-1} \gamma_i)^2 + m^2 c^2}} \right)^2, \quad (\text{S75})$$

where $\boldsymbol{\gamma}$ and c can be further optimized to maximize the ratio.

It will be useful to introduce the cumulative variables

$$\Gamma_j = \frac{\sum_{i=1}^j \gamma_i}{m/2}, \quad (\text{S76})$$

$$\Gamma_j + \Gamma_{j-1} = \frac{\gamma_j + 2 \sum_{i=1}^{j-1} \gamma_i}{m/2}, \quad (\text{S77})$$

and Eq. (S70) becomes

$$\alpha_k = \frac{m^2}{4} (\Gamma_k^2 - \Gamma_{k-1}^2). \quad (\text{S78})$$

With this change of variables, the quantity Δ depends on $\boldsymbol{\gamma}$ only through the sequence $\boldsymbol{\Gamma} = (\Gamma_1, \dots, \Gamma_{m/2})$, so we may regard it as a function of $\boldsymbol{\Gamma}$ and c , and write $\Delta(\boldsymbol{\Gamma}, c)$. In terms of the Γ_j , the ratio can be rewritten as

$$\Delta(\boldsymbol{\Gamma}, c) = \frac{1}{\Gamma_{m/2}^2} \left[2 \sum_{j=1}^{m/2} \frac{(\Gamma_j - \Gamma_{j-1}) \left(\frac{\Gamma_j + \Gamma_{j-1}}{2} \right)^2}{\sqrt{\left(\frac{\Gamma_j + \Gamma_{j-1}}{2} \right)^2 + c^2}} + \left(\sum_{j=1}^{m/2} \frac{(\Gamma_j - \Gamma_{j-1}) c}{\sqrt{\left(\frac{\Gamma_j + \Gamma_{j-1}}{2} \right)^2 + c^2}} \right)^2 \right]. \quad (\text{S79})$$

Let us fix $\Gamma_{m/2} = 1$, and introduce

$$D = \frac{2}{m} \sum_{j=1}^{m/2} \frac{(\Gamma_j - \Gamma_{j-1}) c}{\sqrt{\left(\frac{\Gamma_j + \Gamma_{j-1}}{2} \right)^2 + c^2}}. \quad (\text{S80})$$

We further evaluate the derivative on Γ_j and obtain

$$\begin{aligned} \frac{\partial \Delta}{\partial \Gamma_j} &= \frac{\partial}{\partial \Gamma_j} \left[\frac{(\Gamma_j - \Gamma_{j-1})(\Gamma_j + \Gamma_{j-1})^2}{2\sqrt{\left(\frac{\Gamma_j + \Gamma_{j-1}}{2} \right)^2 + c^2}} + \frac{(\Gamma_{j+1} - \Gamma_j)(\Gamma_{j+1} + \Gamma_j)^2}{2\sqrt{\left(\frac{\Gamma_{j+1} + \Gamma_j}{2} \right)^2 + c^2}} \right] \\ &+ 2 \cdot \frac{m}{2} D \frac{\partial}{\partial \Gamma_j} \left[\frac{(\Gamma_j - \Gamma_{j-1}) c}{\sqrt{\left(\frac{\Gamma_j + \Gamma_{j-1}}{2} \right)^2 + c^2}} + \frac{(\Gamma_{j+1} - \Gamma_j) c}{\sqrt{\left(\frac{\Gamma_{j+1} + \Gamma_j}{2} \right)^2 + c^2}} \right]. \end{aligned} \quad (\text{S81})$$

Let us evaluate the four terms in details

$$\frac{\partial}{\partial \Gamma_j} \left[\frac{(\Gamma_j - \Gamma_{j-1})(\Gamma_j + \Gamma_{j-1})^2}{2\sqrt{\left(\frac{\Gamma_j + \Gamma_{j-1}}{2} \right)^2 + c^2}} \right] = \frac{2(\Gamma_j + \Gamma_{j-1})[c^2(6\Gamma_j - 2\Gamma_{j-1}) + \Gamma_j(\Gamma_j + \Gamma_{j-1})^2]}{[4c^2 + (\Gamma_j + \Gamma_{j-1})^2]^{3/2}}, \quad (\text{S82})$$

$$\frac{\partial}{\partial \Gamma_j} \left[\frac{(\Gamma_{j+1} - \Gamma_j)(\Gamma_{j+1} + \Gamma_j)^2}{2\sqrt{\left(\frac{\Gamma_{j+1} + \Gamma_j}{2} \right)^2 + c^2}} \right] = -\frac{2(\Gamma_j + \Gamma_{j+1})[c^2(6\Gamma_j - 2\Gamma_{j+1}) + \Gamma_j(\Gamma_j + \Gamma_{j+1})^2]}{[4c^2 + (\Gamma_j + \Gamma_{j+1})^2]^{3/2}}, \quad (\text{S83})$$

$$2 \cdot \frac{m}{2} D \frac{\partial}{\partial \Gamma_j} \left[\frac{(\Gamma_j - \Gamma_{j-1}) c}{\sqrt{\left(\frac{\Gamma_j + \Gamma_{j-1}}{2} \right)^2 + c^2}} \right] = md \frac{8c^3 + 4c\Gamma_{j-1}(\Gamma_j + \Gamma_{j-1})}{[4c^2 + (\Gamma_j + \Gamma_{j-1})^2]^{3/2}}, \quad (\text{S84})$$

$$2 \cdot \frac{m}{2} D \frac{\partial}{\partial \Gamma_j} \left[\frac{(\Gamma_{j+1} - \Gamma_j) c}{\sqrt{\left(\frac{\Gamma_{j+1} + \Gamma_j}{2} \right)^2 + c^2}} \right] = -md \frac{4c[2c^2 + \Gamma_{j+1}(\Gamma_j + \Gamma_{j+1})]}{[4c^2 + (\Gamma_j + \Gamma_{j+1})^2]^{3/2}}, \quad (\text{S85})$$

and the derivative is explicitly

$$\begin{aligned} \frac{\partial \Delta}{\partial \Gamma_j} &= \frac{2(\Gamma_j + \Gamma_{j-1})[c^2(6\Gamma_j - 2\Gamma_{j-1}) + \Gamma_j(\Gamma_j + \Gamma_{j-1})^2] + 8c^3md + 4c\Gamma_{j-1}(\Gamma_j + \Gamma_{j-1})md}{[4c^2 + (\Gamma_j + \Gamma_{j-1})^2]^{3/2}} \\ &\quad - \frac{2(\Gamma_j + \Gamma_{j+1})[c^2(6\Gamma_j - 2\Gamma_{j+1}) + \Gamma_j(\Gamma_j + \Gamma_{j+1})^2] + 8c^3md + 4c\Gamma_{j+1}(\Gamma_j + \Gamma_{j+1})md}{[4c^2 + (\Gamma_j + \Gamma_{j+1})^2]^{3/2}}, \end{aligned} \quad (\text{S86})$$

Using $\partial \Delta / \partial \Gamma_j = 0$, we obtain

$$\frac{(\Gamma_j + \Gamma_{j-1})[\Gamma_j(\Gamma_j + \Gamma_{j-1})^2 + c^2(6\Gamma_j - 2\Gamma_{j-1}) + 2c\Gamma_{j-1}md] + 4c^3md}{(\Gamma_j + \Gamma_{j+1})[\Gamma_j(\Gamma_j + \Gamma_{j+1})^2 + c^2(6\Gamma_j - 2\Gamma_{j+1}) + 2c\Gamma_{j+1}md] + 4c^3md} = \frac{[4c^2 + (\Gamma_j + \Gamma_{j-1})^2]^{3/2}}{[4c^2 + (\Gamma_j + \Gamma_{j+1})^2]^{3/2}}. \quad (\text{S87})$$

which gives the algebra equation to solve Γ_j . We also play with the same trick that we relax c and d as free parameters first. We show analytical results with small $m = 2$, $m = 4$, and 6 in the following.

For $m = 2$, we fix $\Gamma_1 = 1$, and we simplify the ratio into

$$\Delta(c) = \frac{1}{\sqrt{1+4c^2}} + \frac{4c^2}{1+4c^2}. \quad (\text{S88})$$

We find the optimal $c = \sqrt{3}/2$. The maximum ratio and the corresponding Bell inequality are

$$\Delta_{\infty,2}^{\max} = 5/4, \quad \boldsymbol{\gamma}^* = (1, 1), \quad \boldsymbol{\alpha}^* = (-1, 1). \quad (\text{S89})$$

For $m = 4$, we fix $\Gamma_2 = 1$, and we simplify the ratio into

$$\Delta(\Gamma_1, c) = \frac{\Gamma_1^3}{\sqrt{\Gamma_1^2 + 4c^2}} + \frac{(1 - \Gamma_1)(1 + \Gamma_1)^2}{\sqrt{(1 + \Gamma_1)^2 + 4c^2}} + 4c^2 \left(\frac{\Gamma_1}{\sqrt{\Gamma_1^2 + 4c^2}} + \frac{(1 - \Gamma_1)}{\sqrt{(1 + \Gamma_1)^2 + 4c^2}} \right)^2. \quad (\text{S90})$$

We find the optimal $\Gamma_1 = 15/34$, and $c = 15^{3/2}/68$. The maximum ratio and the corresponding Bell inequality are

$$\Delta_{\infty,4}^{\max} = 353/272, \quad \boldsymbol{\gamma}^* = \left(\frac{19}{17}, \frac{15}{17}, \frac{15}{17}, \frac{19}{17} \right), \quad \boldsymbol{\alpha}^* = \left(-\frac{931}{289}, -\frac{225}{289}, \frac{225}{289}, \frac{931}{289} \right). \quad (\text{S91})$$

For $m = 6$, we fix $\Gamma_3 = 1$, and simplify the ratio into

$$\begin{aligned} \Delta(\Gamma_1, \Gamma_2, c) &= \frac{\Gamma_1^3}{\sqrt{\Gamma_1^2 + 4c^2}} + \frac{(\Gamma_2 - \Gamma_1)(\Gamma_2 + \Gamma_1)^2}{\sqrt{(\Gamma_2 + \Gamma_1)^2 + 4c^2}} + \frac{(1 - \Gamma_2)(1 + \Gamma_2)^2}{\sqrt{(1 + \Gamma_2)^2 + 4c^2}} \\ &\quad + 4c^2 \left(\frac{\Gamma_1}{\sqrt{\Gamma_1^2 + 4c^2}} + \frac{(\Gamma_2 - \Gamma_1)}{\sqrt{(\Gamma_2 + \Gamma_1)^2 + 4c^2}} + \frac{(1 - \Gamma_2)}{\sqrt{(1 + \Gamma_2)^2 + 4c^2}} \right)^2. \end{aligned} \quad (\text{S92})$$

We find the optimal

$$\Gamma_1 = \frac{1225}{4251}, \quad \Gamma_2 = \frac{2590}{4251}, \quad c = \frac{35^{5/2}}{8502}. \quad (\text{S93})$$

The maximum ratio and the corresponding Bell inequality are

$$\begin{aligned} \Delta_{\infty,6}^{\max} &= \frac{66637}{51012}, \quad \boldsymbol{\gamma}^* = \left(\frac{1661}{1417}, \frac{105}{1417}, \frac{1225}{1417}, \frac{1225}{1417}, \frac{105}{1417}, \frac{1661}{1417} \right), \\ \boldsymbol{\alpha}^* &= \left(-\frac{11362901}{2007889}, -\frac{3675}{1417}, -\frac{1500625}{2007889}, \frac{1500625}{2007889}, \frac{3675}{1417}, \frac{11362901}{2007889} \right). \end{aligned} \quad (\text{S94})$$

B. General odd m

To ensure that more vertices saturate the classical bound, we require that

$$g^* = -\frac{4}{m^2} \left[\left(\frac{\gamma_0}{2} + \sum_{i=1}^k \gamma_i \right)^2 + \sum_{j=k+1}^{(m-1)/2} \alpha_j \right], \quad \text{for any } 0 \leq k \leq (m-1)/2, \quad (\text{S95})$$

from which we solve α_k as

$$\alpha_k = (\gamma_0 + 2 \sum_{i=1}^k \gamma_i) \gamma_k - \gamma_k^2. \quad (\text{S96})$$

The classical bound follows as $g^* = -4 \left(\gamma_0/2 + \sum_{i=1}^{(m-1)/2} \gamma_i \right)^2 / m^2$. For the quantum value, we simplify

$$f(\mathbf{s}) = -\frac{4}{m^2} \left\{ \sum_{j=1}^{(m-1)/2} [\gamma_0 \gamma_j + 2 \gamma_j (\sum_{i=1}^j \gamma_i) - \gamma_j^2] s_j + \left(\frac{\gamma_0}{2} + \sum_{j=1}^{(m-1)/2} \gamma_j \sqrt{1 - s_j^2} \right)^2 \right\}. \quad (\text{S97})$$

The optimal s_j is given by

$$s_j^* = \left[1 + \frac{m^2 c^{*2}}{(\gamma_0 + \gamma_j + 2 \sum_{i=1}^{j-1} \gamma_i)^2} \right]^{-1/2}. \quad (\text{S98})$$

We relax c as a free parameter, and obtain the ratio as

$$\begin{aligned} \Delta(\boldsymbol{\gamma}, c) &= \sum_{j=1}^{(m-1)/2} \frac{1}{\left(\frac{\gamma_0}{2} + \sum_{i=1}^{(m-1)/2} \gamma_i \right)^2} \frac{\left[\gamma_0 + \gamma_j + 2 \left(\sum_{i=1}^{j-1} \gamma_i \right) \right]^2 \gamma_j}{\sqrt{(\gamma_0 + \gamma_j + 2 \sum_{i=1}^{j-1} \gamma_i)^2 + m^2 c^2}} \\ &+ \left(\frac{\gamma_0}{2 \left(\frac{\gamma_0}{2} + \sum_{i=1}^{(m-1)/2} \gamma_i \right)} + \sum_{j=1}^{(m-1)/2} \frac{\gamma_j}{\frac{\gamma_0}{2} + \sum_{i=1}^{(m-1)/2} \gamma_i} \frac{mc}{\sqrt{(\gamma_0 + \gamma_j + 2 \sum_{i=1}^{j-1} \gamma_i)^2 + m^2 c^2}} \right)^2. \end{aligned} \quad (\text{S99})$$

We introduce the cumulative variables

$$\Gamma_j = \frac{2}{m} \left(\frac{\gamma_0}{2} + \sum_{i=1}^j \gamma_i \right), \quad (\text{S100})$$

$$\Gamma_0 = \frac{2}{m} \frac{\gamma_0}{2}, \quad (\text{S101})$$

and Eq. (S96) becomes

$$\alpha_k = \frac{m^2}{4} (\Gamma_k^2 - \Gamma_{k-1}^2). \quad (\text{S102})$$

Similarly to the case with even m , we rewrite the ratio into

$$\Delta(\boldsymbol{\Gamma}, c) = \frac{1}{\Gamma_{(m-1)/2}^2} \left[2 \sum_{j=1}^{(m-1)/2} \frac{\left(\frac{\Gamma_j + \Gamma_{j-1}}{2} \right)^2 (\Gamma_j - \Gamma_{j-1})}{\sqrt{\left(\frac{\Gamma_j + \Gamma_{j-1}}{2} \right)^2 + c^2}} + \left(\Gamma_0 + \sum_{j=1}^{(m-1)/2} \frac{c(\Gamma_j - \Gamma_{j-1})}{\sqrt{\left(\frac{\Gamma_j + \Gamma_{j-1}}{2} \right)^2 + c^2}} \right)^2 \right]. \quad (\text{S103})$$

We fix $\Gamma_{(m-1)/2} = 1$. For $m = 3$, we obtain

$$\Delta(\boldsymbol{\Gamma}_0, c) = 2 \frac{\left(\frac{1+\Gamma_0}{2} \right)^2 (1 - \Gamma_0)}{\sqrt{\left(\frac{1+\Gamma_0}{2} \right)^2 + c^2}} + \left(\Gamma_0 + \frac{c(1 - \Gamma_0)}{\sqrt{\left(\frac{1+\Gamma_0}{2} \right)^2 + c^2}} \right)^2. \quad (\text{S104})$$

We find the optimal

$$\Gamma_0 = 2/7, c = 6/7. \quad (\text{S105})$$

The maximum ratio and the corresponding Bell inequality are

$$\Delta_{\infty,3}^{\max} = 9/7, \boldsymbol{\gamma}^* = \left(\frac{15}{14}, \frac{6}{7}, \frac{15}{14} \right), \boldsymbol{\alpha}^* = \left(-\frac{405}{196}, 0, \frac{405}{196} \right). \quad (\text{S106})$$

For $m = 5$, we obtain

$$\Delta(\Gamma_0, \Gamma_1, c) = \frac{(\Gamma_1 + \Gamma_0)^2(\Gamma_1 - \Gamma_0)}{\sqrt{(\Gamma_1 + \Gamma_0)^2 + 4c^2}} + \frac{(1 + \Gamma_1)^2(1 - \Gamma_1)}{\sqrt{(1 + \Gamma_1)^2 + 4c^2}} + \left(\Gamma_0 + \frac{c(\Gamma_1 - \Gamma_0)}{\sqrt{(\frac{\Gamma_1 + \Gamma_0}{2})^2 + c^2}} + \frac{c(1 - \Gamma_1)}{\sqrt{(\frac{1 + \Gamma_1}{2})^2 + c^2}} \right)^2. \quad (\text{S107})$$

We find the optimal

$$\Gamma_0 = \frac{36}{211}, \quad \Gamma_1 = \frac{114}{211}, \quad c = \frac{180}{211}. \quad (\text{S108})$$

The maximum ratio and the corresponding Bell inequality are

$$\Delta_{\infty, 5}^{\max} = \frac{275}{211}, \quad \boldsymbol{\gamma}^* = \left(\frac{485}{422}, \frac{195}{211}, \frac{180}{211}, \frac{195}{211}, \frac{485}{422} \right), \quad \boldsymbol{\alpha}^* = \left(-\frac{788125}{178084}, -\frac{73125}{44521}, 0, \frac{73125}{44521}, \frac{788125}{178084} \right). \quad (\text{S109})$$

C. $m \rightarrow \infty$ limit

When $m \rightarrow \infty$, we represent the discrete sequences $\{\alpha_j\}$, $\{\gamma_j\}$ and $\{s_j\}$ by smooth functions $\alpha(u)$, $\gamma(u)$ and $s(u)$ on $[0, 1]$, defined via $\alpha_j = m\alpha(2j/m)$, $\gamma_j = \gamma(2j/m)$, and $s_j = s(2j/m)$. The previous definition of Γ_j then becomes

$$\Gamma_j = \frac{\sum_{i=1}^j \gamma_i}{m/2} = \frac{\sum_{i=1}^j \gamma(2i/m)}{m/2} \approx \int_0^{2j/m} \gamma(u) du. \quad (\text{S110})$$

We simplify the classical bound as a functional of $s(u)$:

$$g[s(u)] = - \int_0^1 2\alpha(u)s(u) du - \iint_0^1 du du' \gamma(u)\gamma(u') [1 - \max(s(u), s(u'))]. \quad (\text{S111})$$

Using the fact that the optimal $s(u)$ takes only the values 0 or 1, we write $E = \{u \in [0, 1] : s(u) = 1\}$ and obtain

$$g[s(u)] = - \int_E 2\alpha(u) du - \left(\int_{E^c} \gamma(u) du \right)^2, \quad (\text{S112})$$

where E^c is the complement of E .

The quantum value is related to the functional

$$f[s(u)] = - \int_0^1 2\alpha(u)s(u) du - \left(\int_0^1 \gamma(u)\sqrt{1 - s(u)^2} du \right)^2, \quad (\text{S113})$$

where $s(u)$ satisfies the constraint $0 \leq s(u) \leq 1$, and we denote

$$c = \int_0^1 \gamma(u)\sqrt{1 - s(u)^2} du. \quad (\text{S114})$$

The optimal $s^*(u)$ is

$$s^*(u) = \frac{1}{\sqrt{1 + c^2\gamma(u)^2/\alpha(u)^2}}, \quad (\text{S115})$$

and the self-consistency condition for c becomes

$$\int_0^1 \frac{\gamma(u)^2}{\sqrt{\alpha(u)^2 + c^2\gamma(u)^2}} du = 1. \quad (\text{S116})$$

We maximize the ratio Δ by optimizing the functional forms of $\alpha(u)$ and $\gamma(u)$. The optimal choice of $\alpha(u)$ follows from Eqs. (S70) and (S96) as

$$\alpha(u) = \gamma(u) \int_0^u \gamma(v) dv. \quad (\text{S117})$$

The corresponding optimal classical bound is

$$g^* = - \left[\int_0^1 \gamma(u) du \right]^2. \quad (\text{S118})$$

With $\alpha(u)$ given by Eq. (S117), the quantum value is related to

$$f[s(u), \gamma(u)] = -2 \int_0^1 du \int_0^u dv \gamma(u) \gamma(v) s(u) - \left(\int_0^1 \gamma(u) \sqrt{1 - s(u)^2} du \right)^2, \quad (\text{S119})$$

by choosing

$$s^*(u) = \frac{1}{\sqrt{1 + c^{*2} / [\int_0^u \gamma(v) dv]^2}}. \quad (\text{S120})$$

Substituting the optimal $s^*(u)$ into $f[s(u)]$, we obtain

$$f^*[\gamma(u)] = -2 \int_0^1 du \int_0^u dv \int_0^u dw \frac{\gamma(w) \gamma(u) \gamma(v)}{\sqrt{[\int_0^u \gamma(w) dw]^2 + c^{*2}}} - \left(\int_0^1 du \frac{c^* \gamma(u)}{\sqrt{[\int_0^u \gamma(w) dw]^2 + c^{*2}}} \right)^2. \quad (\text{S121})$$

Since the denominator depends only on u , the integrations over v and w simply yield $(\int_0^u \gamma(v) dv)^2$. Introducing the cumulative function

$$\Gamma(u) = \int_0^u \gamma(v) dv, \quad \Gamma'(u) = \gamma(u), \quad (\text{S122})$$

we can rewrite Eq. (S121) as a functional of $\Gamma(u)$:

$$f^*[\Gamma(u)] = -2 \int_0^1 du \frac{\Gamma(u)^2 \Gamma'(u)}{\sqrt{\Gamma(u)^2 + c^{*2}}} - \left(\int_0^1 du \frac{c^* \Gamma'(u)}{\sqrt{\Gamma(u)^2 + c^{*2}}} \right)^2. \quad (\text{S123})$$

Assuming that $\Gamma(u)$ is monotonic so that the change of variables $\Gamma = \Gamma(u)$ is valid, and denoting $\Gamma_f := \Gamma(1)$, Eq. (S123) is equivalently

$$f^*[\Gamma] = -2 \int_0^{\Gamma_f} d\Gamma \frac{\Gamma^2}{\sqrt{\Gamma^2 + c^{*2}}} - \left(\int_0^{\Gamma_f} d\Gamma \frac{c^*}{\sqrt{\Gamma^2 + c^{*2}}} \right)^2. \quad (\text{S124})$$

In the continuum limit $m \rightarrow \infty$, the discrete expressions (S79) and (S103) for the ratio Δ also reduce to an integral that depends only on the final cumulative value $\Gamma_{m/2} = \Gamma_f$. The ratio is explicitly

$$\Delta(\Gamma_f, c) = \frac{1}{\Gamma_f^2} \left[2 \int_0^{\Gamma_f} \frac{\Gamma^2}{\sqrt{\Gamma^2 + c^2}} d\Gamma + \left(\int_0^{\Gamma_f} \frac{c}{\sqrt{\Gamma^2 + c^2}} d\Gamma \right)^2 \right]. \quad (\text{S125})$$

Thus, in the continuum limit both the optimal quantum value and the classical bound depend on $\gamma(u)$ only through the final cumulative parameter Γ_f , and the ratio Δ is fully characterized by the one-dimensional integral in Eq. (S125). We fix $\Gamma_{m/2} = 1$ and complete the integral to obtain

$$\Delta_{\infty, \infty}(c) = \sqrt{1 + c^2} + c^2 [\coth^{-1}(\sqrt{1 + c^2})^2 - \coth^{-1}(\sqrt{1 + c^2})]. \quad (\text{S126})$$

The maximum ratio is

$$\Delta_{\infty, \infty}^{\max} = \coth(1), \quad (\text{S127})$$

which is reached by

$$c^* = 1/\sinh(1). \quad (\text{S128})$$

D. Optimizing α_k for uniform weights $\gamma_k = 1$

Here we consider the situation with fixed $\gamma_k = 1$ and optimize only over α_k , which corresponds to the setting studied in Ref. [S7]. From Eqs. (S96) and (S70) we obtain

$$\alpha_k = 2k \quad \text{for odd } m, \quad \alpha_k = 2k - 1 \quad \text{for even } m.$$

In this case the expression for the ratio simplifies to

$$\Delta(\mathbf{1}, c) = \begin{cases} \sum_{j=1}^{m/2} \frac{4}{m^2} \frac{(2j-1)^2}{\sqrt{(2j-1)^2 + m^2 c^2}} + \left(\sum_{j=1}^{m/2} \frac{2c}{\sqrt{(2j-1)^2 + m^2 c^2}} \right)^2, & \text{even } m, \\ \sum_{j=1}^{(m-1)/2} \frac{4}{m^2} \frac{4j^2}{\sqrt{4j^2 + m^2 c^2}} + \left(\frac{1}{m} + \sum_{j=1}^{(m-1)/2} \frac{2c}{\sqrt{4j^2 + m^2 c^2}} \right)^2, & \text{odd } m. \end{cases} \quad (\text{S129})$$

In Table 3 of the main text, the values of the ratio for finite m and fixed $\gamma = \mathbf{1}$ are obtained from Eq. (S129) by numerically maximizing $\Delta(\mathbf{1}, c)$ over c . In the large- m limit the sums in Eq. (S129) can be replaced by integrals, and one recovers the continuum expression in Eq. (S125) with $\Gamma_f = 1$.

[S1] J. Tura, R. Augusiak, A. B. Sainz, T. Vértesi, M. Lewenstein, and A. Acín, *Science* **344**, 1256 (2014).
 [S2] E. H. Moore, *Bull. Amer. Math. Soc.* **26**, 394 (1920).
 [S3] R. Penrose, *Mathematical Proceedings of the Cambridge Philosophical Society* **51**, 406 (1955).
 [S4] L. J. Landau, *Foundations of Physics* **18**, 449 (1988).
 [S5] L. Masanes, “Necessary and sufficient condition for quantum-generated correlations,” (2003), arXiv:quant-ph/0309137.
 [S6] K. Fukuda, “Cddlib reference manual,” (2003).
 [S7] S. Wagner, R. Schmied, M. Fadel, P. Treutlein, N. Sangouard, and J.-D. Bancal, *Physical Review Letters* **119**, 170403 (2017).